



FLEXKB DOCUMENT
Version: HI.001.01242019.73032
Document generated: 01/24/2019

CISNET ESOPHAGUS CANCER COLLABORATORS

Important note: This document will remain archived as a technical appendix for publications. New versions will be added periodically as model refinements and updates are completed. The most current version is available at <http://cisnet.cancer.gov/profiles>. The CISNET model profile topics are not necessarily meant to be read in sequential fashion, so the reader should feel free to skip around as their interests dictate.

We recommend you let your interests guide you through this document, using the navigation tree as a general guide to the content available.

The intent of this document is to provide the interested reader with insight into ongoing research. Model parameters, structure, and results contained herein should be considered representative but preliminary in nature.

We encourage interested readers to contact the contributors for further information.

 COLUMBIA COLUMBIA UNIVERSITY IRVING MEDICAL CENTER	Columbia University Irving Medical Center (EACMo)
 UNIVERSITY of WASHINGTON ErasmusMC	Erasmus/University of Washington (MISCAN-ESO)
 FRED HUTCHINSON CANCER RESEARCH CENTER A LIFE OF SCIENCE	Fred Hutchinson Cancer Research Center (MSCE-EAC)



FLEXKB DOCUMENT
Version: HI.001.01242019.73031
Document generated: 01/24/2019

COLUMBIA UNIVERSITY IRVING MEDICAL CENTER



[Readers Guide](#)
[Model Overview](#)
[Assumption Overview](#)
[Parameter Overview](#)
[Component Overview](#)
[Output Overview](#)
[Results Overview](#)
[Key References](#)

Important note: This document will remain archived as a technical appendix for publications. New versions will be added periodically as model refinements and updates are completed. The most current version is available at <http://cisnet.cancer.gov/profiles>. The CISNET model profile topics are not necessarily meant to be read in sequential fashion, so the reader should feel free to skip around as their interests dictate.

We recommend you let your interests guide you through this document, using the navigation tree as a general guide to the content available.

The intent of this document is to provide the interested reader with insight into ongoing research. Model parameters, structure, and results contained herein should be considered representative but preliminary in nature.

We encourage interested readers to contact the contributors for further information.

Go directly to the: [Reader's Guide](#).



READERS GUIDE

CORE PROFILE DOCUMENTATION

These topics will provide an overview of the model without the burden of detail. Each can be read in about 5–10 minutes. Each contains links to more detailed information if required.



Readers Guide
Model Overview
Assumption Overview
Parameter Overview
Component Overview
Output Overview
Results Overview
Key References

Model Purpose

This document describes the primary purpose of the model.

Model Overview

This document describes the primary aims and general purposes of this modeling effort.

Assumption Overview

An overview of the basic assumptions inherent in this model.

Parameter Overview

Describes the basic parameter set used to inform the model, more detailed information is available for each specific parameter.

Component Overview

A description of the basic computational building blocks (components) of the model.

Output Overview

Definitions and methodologies for the basic model outputs.

Results Overview

A guide to the results obtained from the model.

Key References

A list of references used in the development of the model.



MODEL PURPOSE

SUMMARY

The primary purpose of the esophageal adenocarcinoma model (EACMo) is to advance our understanding of esophageal adenocarcinoma (EAC), including its natural history in order to positively impact cancer control. A particular interest is the management of Barrett's esophagus, a pre-malignant condition associated with high risk of developing EAC, which has become a significant clinical management issue with increasing upper endoscopy utilization.

PURPOSE

Since 1975 the incidence of EAC in the United States has seen a more than six-fold increase. In light of this alarming trend, EACMo was developed to advance our understanding of this disease. The model includes a natural history component, as well as screening and intervention components.

The purpose of the natural history component is to systematically integrate and synthesize all available information about the progression of the disease. EACMo includes a calibrated Markov state transition model of EAC, including precursor health states such as GERD, Barrett's esophagus (BE), and dysplasia; this model agrees well with available data on EAC incidence and mortality, as well as with published rates of BE and GERD prevalence. The natural history model includes age, period, and cohort effects, and can be used to explore and analyze different hypotheses as to the cause of the rise in EAC incidence. It has been used to produce projections of EAC incidence into the future.¹ Finally, the natural history model serves as a foundation upon which we can overlay and assess the impact of screening or other interventions.

In addition to the natural history of the disease, EACMo seeks to evaluate the effectiveness of current practice in screening for EAC and managing precursor states such as BE. To accomplish this, EACMo's design includes screening and treatment components which can be tailored for each specific analysis. Specific questions which EACMo has been used to address or may be used to address in the future include:

1. What is the effectiveness of current endoscopic practice in terms of surveillance of BE patients?
2. What is the practicality of targeted screening based on biomarkers or other identifiable risk factors?
3. What is the impact and effectiveness of radiofrequency ablation as a treatment for non-dysplastic or dysplastic BE?
4. What are the chemopreventive effects of aspirin or other medications?
5. What is the impact of early detection of EAC with new endoscopic technologies?

Future plans for EACMo include its use in the development of decision aids.

REFERENCES:

- ¹ Kong CY, Kroep S, Curtius K, Hazelton WD, Jeon J, Meza R, Heberle CR, Miller MC, Choi SE, Lansdorp-Vogelaar I, van Ballegooijen M, Feuer EJ, Inadomi JM, Hur C, Luebeck EG "Exploring the recent trend in esophageal adenocarcinoma incidence and mortality using comparative simulation modeling." in *Cancer Epidemiol Biomarkers Prev.* 2014; 23: 6: 997-1006



MODEL OVERVIEW

SUMMARY

This document provides a broad overview of EACMo, including information about its basic structure and the kinds of problems it was designed to solve.



PURPOSE

The purpose of the model is to inform our understanding of esophageal cancer, its natural history, and the efficacy of screening and other interventions.

BACKGROUND

Since 1975 there has been a rapid (more than six-fold) rise in EAC incidence in the United States. Given this increase, and the high mortality associated with advanced stages of the disease, it is imperative to explore approaches to prevention or early detection to reduce the burden of the disease.

Even with this dramatic increase, the absolute number of EAC cases per year remains too low to screen the general population,¹ although targeted endoscopic screening may be appropriate. Heartburn, the primary symptom of gastroesophageal reflux disease (GERD), affects 60 million Americans² and can lead to Barrett's esophagus (BE), a pre-malignant condition associated with the greatest risk (30–125x) of developing EAC.³ Because of the significant number of individuals affected by GERD and BE, the management of these patients has become a public health issue, recently underscored by an Institute of Medicine report that prioritized crucial areas for comparative effectiveness research.⁴ However, the relatively low rate of progression to cancer⁵ has made clinical trials with cancer endpoints challenging because of the number of subjects and follow-up period required. These difficulties have contributed to the lack of an accepted screening and management strategy.

EACMo has numerous precursor model versions including clinical or patient-centered models of Barrett's esophagus that focused on specific clinical issues such as the management of high-grade dysplasia and chemoprevention with aspirin as examples. However, EACMo is different and more comprehensive as it is a population model that fully leverages the US SEER cancer data registry. Thus, the model is now equipped to assess screening, surveillance and prevention strategies for population cancer control.

MODEL DESCRIPTION

EACMo represents the natural history of esophageal adenocarcinoma as a state-transition model. It models the progression of a population through health states including normal health, BE, dysplasia, preclinical cancer, clinical cancer, and death. Screening and treatment can be imposed on top of this natural history model to estimate their potential impact.

The natural history component of EACMo is a Markov model with a cycle length of one month. Transition rates depend on age, and may also depend on birth cohort and/or calendar year. Transition rates which cannot be determined directly from empirical data are calibrated. Model parameters are calibrated separately for white male, all male, white female, and all female versions of the model. Given the large number of



parameters, a [simulated annealing algorithm](#) is used to efficiently search the parameter space and determine the optimum values in an automated fashion.

EACMo's natural history component supports simulation at both the population and individual levels of analysis. When simulating individuals during screening and treatment components, the model transitions from a semi-Markov population model to a microsimulation model to account for transitions that depend on an individual patient's history beyond the most recent health state. This allows us to conduct analyses with a high degree of clinical realism while keeping the core of EACMo as simple as possible.

Primary calibration inputs are SEER EAC incidence and mortality data, by age, gender, and calendar year. Additional inputs for calibration include estimates of GERD prevalence and of BE prevalence.

Inputs for the calibrated model are primarily the calibrated transition parameters, which include parameters for age-dependent transition functions as well as functions of birth year and of calendar year. Other inputs include initial values for BE and GERD prevalence, population tables, and life tables for including all source mortality.

Primary outputs are incidence and incidence-based mortality of EAC, including future projections. Secondary outputs include prevalence of GERD, BE, including dysplasia. Other outputs which have been or can be computed from the model include life years/expectancy, cancer progression/dwell time, progression rates, costs, and measures of the impact of screening and medical efficiency such as the number of endoscopies needed to prevent one cancer in a given population.

We have sought to attain a high degree of transparency via a simple model design; consequently, some aspects of the model may be oversimplified relative to clinical reality. (See [Assumption Overview](#) for more details.) Additionally, data pertaining to the natural history of EAC, particularly precursor states, remain sparse, making it difficult to estimate needed calibration targets such as the prevalence of BE as a function of calendar year stratified by age and gender.

REFERENCES:

- ¹ Ries LAG, Melbert D, Krapcho M, Stinchcomb DG, Howlader N, et al. "SEER Cancer Statistics Review, 1975-2005" 2008;
- ² Locke GR, 3rd, Talley NJ, Fett SL, Zinsmeister AR, Melton LJ, 3rd. "Prevalence and clinical spectrum of gastroesophageal reflux: a population-based study in Olmsted County, Minnesota." in *Gastroenterology* 1997; 112: 5: 1448-56
- ³ Williamson WA, Ellis FH Jr, Gibb SP, Shahian DM, Aretz HT, Heatley GJ, Watkins E Jr. "Barrett's esophagus. Prevalence and incidence of adenocarcinoma." in *Archives of Internal Medicine* 1991; 151: 11: 2212-6
- ⁴ Institute of Medicine "Initial National Priorities for Comparative Effectiveness Research" 2009;
- ⁵ Shaheen NJ, Crosby MA, Bozyski EM, Sandler RS "Is there publication bias in the reporting of cancer risk in Barrett's esophagus? " in *Gastroenterology* 2000; 119: 2: 333-8



ASSUMPTION OVERVIEW

SUMMARY

This document provides an overview of the major assumptions made in constructing EACMo.



BACKGROUND

Although SEER provides extensive data on EAC incidence and mortality, data on EAC's precursor health states, including GERD, BE, and dysplasia, are relatively sparse. Thus, any model of EAC will involve significant assumptions about the natural history of the disease. In developing EACMo, assumptions were chosen with two goals in mind: keep the model structure as simple as possible, and maximize the utility of the high quality data that does exist.

ASSUMPTION LISTING

No Regression

We assume that there is no 'regression' between health states. In particular, patients with dysplasia cannot return to BE with no dysplasia (or to a lower grade of dysplasia) without treatment, and likewise patients with Barrett's esophagus do not spontaneously regress to normal health. The extent to which regression from these states occurs in the real world is unclear as there are reports in the clinical literature. Omitting regression is an example of prioritizing model simplicity in the lack of definitive evidence.

Markov Property

In the natural history model we assume that a patient's health state depends only on their state in the previous cycle. Thus, for example, a patient who has been in the BE health state for one year has the same probability of transitioning to cancer as a patient who has had BE for 10 years (provided they are the same age, gender, etc.). This is a key simplifying assumption that makes automatic calibration feasible. It is important to note that this assumption applies only to the natural history of the disease in the model; screening and treatment strategies can take into account details of the patient's full history.

Calibration Constraints

Calibration to SEER data is the process used to systematically fill in the gaps in our knowledge of the disease natural history. Several assumptions based on the published literature were made to constrain the parameter space for the calibration process. These include constraints on the relative transition rates from normal to BE vs GERD to BE, the ratio of short vs long segment BE, and the progression rates out of short vs long segment BE. More detail on these assumptions can be found in the component overview document under the calibration component.



PARAMETER OVERVIEW

SUMMARY

This document provides a high level description of the parameters used in EACMo.

BACKGROUND

Data pertaining to the natural history of EAC is generally quite limited, due to the rarity of the disease and the low progression rate from identifiable precancerous states. However, the Surveillance Epidemiology and End Results (SEER) registry provides data on the incidence and mortality of EAC (including stage distribution) in the U.S. population, stratified by age, year of diagnosis, gender, and race, from ages 20 to 84 and calendar years 1975 to 2010. EACMo is designed to leverage this high-quality data as much as possible. Additionally, estimates of GERD prevalence and BE prevalence over time are drawn from the literature. The actual parameters are determined by calibration to produce outputs matching the known values, with an emphasis on agreement with SEER data.

Analyses of screening or treatment require additional parameters to realistically model the strategies being tested. Examples are provided in the parameter listing below. These parameters are estimated as needed from clinical studies in the published literature, including additional patient-level data when available directly from researchers when possible. When such clinical study is not available, we may rely on estimates based on both expert opinion and biologic plausibility. Sensitivity analyses can be conducted to incorporate the uncertainty in these parameters and assess potential impact on model results.

PARAMETER LISTING OVERVIEW

Natural History Parameters

Most parameters in the natural history model are used to determine the probability of transitioning from one state to another. For a few transitions, this probability can be computed directly from available data. For example, the transition probability from any state to non-cancer-related death can be taken directly from available life tables, and the transition probabilities from detected cancer states to cancer mortality can be inferred from SEER survival data.

All other transition rates are determined by parameter calibration. In general multiple parameters may be needed to compute a single transition rate. Parameters may be logically divided into those pertaining to age, calendar year, and birth cohort. Age is assumed to be the predominant effect; in the current model, all transition rates increase as a linear function (determined by two calibrated parameters) of the patient's age. Period and cohort effects are secondary and are only applied to certain transitions. Currently all period and cohort effects are modeled as logistic functions, requiring four parameters each to fit, although other functions are possible. Further understanding of the underlying causes of the rise in EAC will allow us to better inform the period and cohort effects in our model, providing for more confident projections of EAC incidence and mortality.

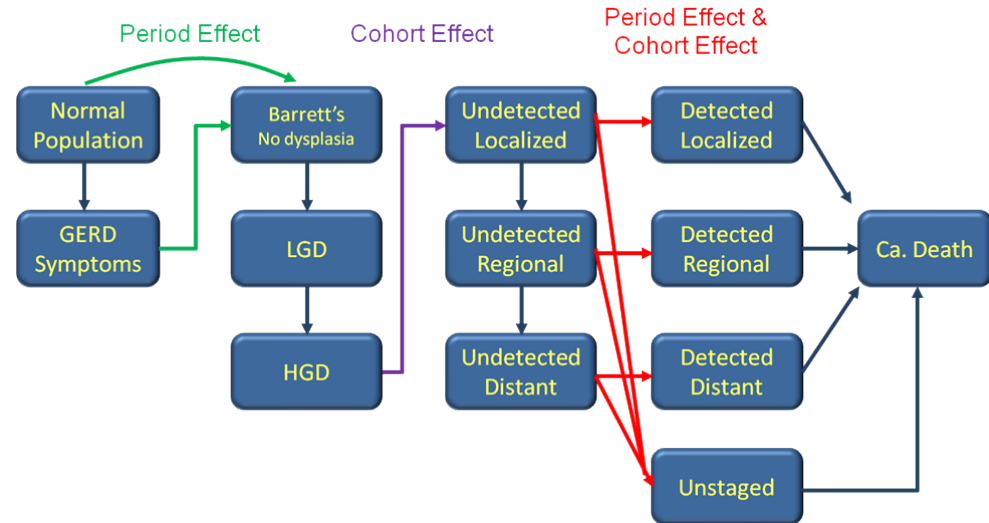
The current model includes a period effect on the rate of transition from Normal and GERD to BE, a cohort effect on the transition from high grade dysplasia to undetected localized EAC, and both period and cohort effects on the transitions from undetected



- Readers Guide
- Model Overview
- Assumption Overview
- Parameter Overview
- Component Overview
- Output Overview
- Results Overview
- Key References

to detected cancer, with the cohort effect from HGD to undetected localized EAC having the largest impact on the increase in EAC incidence over time. This is summarized in the diagram below.

The choice of where to apply period and cohort effects represents important assumptions about the natural history of EAC and the potential causes of its recent rise in incidence. These assumptions merit careful consideration as additional data become available and during the development of the model.



Model Schematic

Parameters for Screening and Other Interventions

When overlaying screening or other interventions on the natural history model it is necessary to obtain estimates of many other parameters. These are generally not determined by calibration but rather taken directly from the literature or estimated by expert opinion. The parameters needed vary widely with the strategy being tested. An incomplete list of examples includes test performance characteristics, recurrence rates after treatment, complication (and mortality) rates for a particular treatment or screening method, costs of treatment or screening, quality of life adjustments, and efficacy of treatment.

COMPONENT OVERVIEW

SUMMARY

This document describes the components of EACMo.

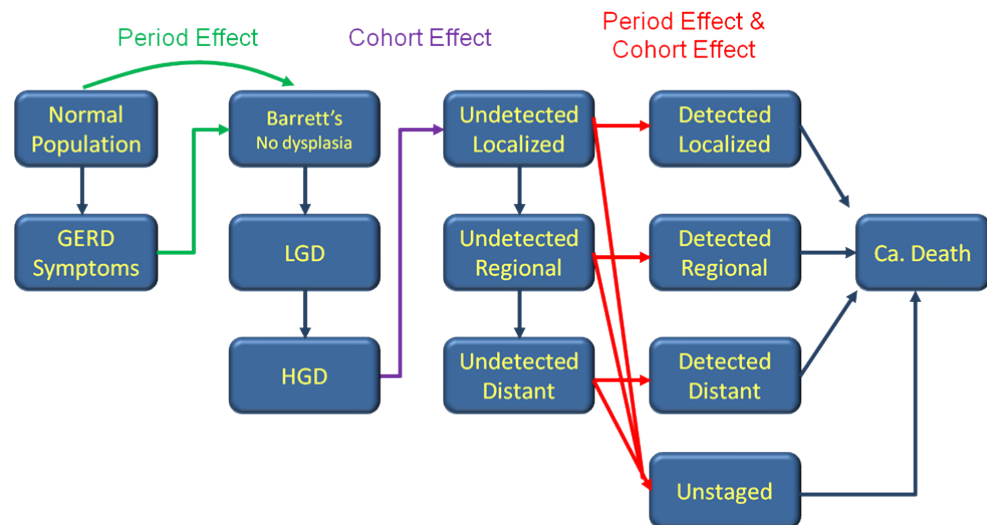
OVERVIEW

Natural History Component

Simulated populations enter the model in the Normal Population state and may pass through up to five additional health states. Fractions of the population can progress from the Normal State to the GERD symptomatic state (or directly to the BE state) and fractions of this second state can further progress to the BE state. Increasingly smaller populations then progress from BE to Undetected Cancer and Detected Cancer, and finally Death. A simplified schematic of the natural history model is shown below. The natural history component supports both population-level and individual-level simulation.



- Readers Guide
- Model Overview
- Assumption Overview
- Parameter Overview
- Component Overview
- Output Overview
- Results Overview
- Key References



Model Schematic

Calibration Component

The calibration component is responsible for determining the optimum parameters for the Natural History Component. It uses a simulated annealing algorithm to efficiently and automatically find the natural history transition rates that produce output best aligned or optimally calibrated to SEER data.

Screening/Intervention Components

These components interact with the calibrated natural history model, overlaying the strategy to be tested and allowing its health impact to be measured. These simulate patients at the individual level, allowing for a high degree of clinical realism. They can be customized for each individual analysis.

COMPONENT LISTING

Natural History Component

This is the core component of EACMo; it simulates the natural history of EAC from normal health through GERD, BE, Undetected Cancer, Detected Cancer, and Death. Transition rates between states are determined by the calibration component, which



automatically chooses the values which optimize the model fit to SEER data.

Patients enter the model in the Normal state at age 20 and may progress directly to BE, or may progress to the GERD state and then to BE.

The BE state consists of six subdivisions (clinical factors) by length and dysplasia status: Short segment BE (SSBE) with no dysplasia (ND), with low grade dysplasia (LGD), and with high grade dysplasia (HGD), and long segment BE (LSBE) with the same dysplasia classifications. These subdivisions are important because dysplasia status and BE segment length are known predictors of risk of progression to cancer; a patient with high grade dysplasia warrants a different management strategy for their condition than a patient with BE alone. Patients in the no dysplasia states may progress to either LGD or directly to HGD. From the HGD subcomponents patients may progress to undetected localized cancer.

From undetected localized cancer patients may progress to regional cancer, and from there to distant. At each stage there is a probability of progressing to detected cancer.

We assume that all cancer patients must first pass through BE (both non dysplasia and HGD), that there are no transitions from short segment BE subcomponents to long segment BE subcomponents or vice versa, and that there is no regression among health states. We assume that all transition rates increase with age, while a few transition rates are assumed to depend on calendar year or birth cohort.

Recently, the natural history component has been used – in conjunction with the other CISNET EAC models – to explore the rise in EAC and provide projections of future incidence and mortality.¹

Calibration Component

This component is responsible for setting all transition rates in the natural history component, with the exceptions of all-cause mortality and cancer-specific mortality for patients with detected cancer (which are derived directly from available data). Calibration is necessary because the transition rates can vary by calendar year, age, and birth cohort and there is insufficient data in the literature to estimate these values directly. Therefore, this component uses a simulated annealing approach to efficiently search the parameter space and automatically select an optimum set of transition rates that maximize model fit to clinical targets. The optimum calibrated parameter set can be used to inform estimates of quantities that cannot be measured in a clinical setting, such as mean sojourn times and estimated transition rates between preclinical states.

The search space for this process was constrained by several assumptions. The age-dependent transition rates from normal to no dysplasia were fixed as 1/6 the corresponding rates from GERD to no dysplasia. Likewise, the transition rates from short segment HGD to cancer were fixed as 1/2 the corresponding rates from long segment HGD to cancer. The transitions into long segment and short segment no dysplasia were constrained such that the total ratio of short segment BE to long segment BE is approximately 3:1.

Screening/Intervention Components

These components overlay screening, treatment, or other disease management strategies on top of the natural history model. EACMo uses a ‘parallel universe’ approach; the impact of an intervention is measured by simulating the disease history



in the presence of that intervention, then comparing the outcomes to a simulation of the natural history alone. The specifics of the intervention components vary with each analysis. Costs and health-related quality of life adjustments are common to each CISNET model of esophageal adenocarcinoma, and are therefore handled external to the core of EACMo.

REFERENCES:

- ¹ Kong CY, Kroep S, Curtius K, Hazelton WD, Jeon J, Meza R, Heberle CR, Miller MC, Choi SE, Lansdorp-Vogelaar I, van Ballegooijen M, Feuer EJ, Inadomi JM, Hur C, Luebeck EG "Exploring the recent trend in esophageal adenocarcinoma incidence and mortality using comparative simulation modeling." in *Cancer Epidemiol Biomarkers Prev.* 2014; 23: 6: 997-1006



OUTPUT OVERVIEW

SUMMARY

This document provides an overview of the outputs produced by EACMo.

OVERVIEW

EACMo outputs can be broadly divided into natural history outputs and intervention assessment outputs.

Natural history outputs include incidence and mortality of EAC, prevalence of BE and GERD, progression rates, and dwell time (the time from onset of BE to development of cancer). Outputs in this category can be used for calibration and validation of the model. Additionally, the model can be extrapolated into the future to provide projections of these outputs.

Intervention assessment outputs or clinical endpoints can include number of treatments or endoscopies needed, reduction in cancer mortality, life years gained, and total costs. These outputs relate directly to decisions about treatment/prevention of EAC and management of precursor health states such as BE.

OUTPUT LISTING

EAC Incidence & Mortality

A primary output of the model is the incidence and mortality of EAC, stratified by age, race, gender, and calendar year. The model is calibrated so that the natural history model output agrees with SEER data for the years where such data are available. This output is also available in future projections. When intervention strategies are overlaid on the natural history model, the change in this output is a key endpoint.

BE/Dysplasia Prevalence

An early version of EACMo was used to estimate the prevalence of BE in the U.S. population. In the current model, overall BE prevalence as estimated from the available literature is used as a calibration target. The breakdown of low grade and high grade dysplasia within BE is also constrained during calibration. Estimates of BE and dysplasia prevalence within different subpopulations are important when evaluating the overall costs and benefits of screening, surveillance, and treatment.

Progression Rates/Dwell Time

EACMo can produce various estimates of the time of progression from one health state to another. For example, the 'dwell time' between onsets of BE and development of EAC can be estimated. These timings are of clinical significance, and are useful for model validation and comparison to other models.

Costs/Efficiency Estimates

The cost of an intervention is of obvious importance to health policy planning. These costs can be aggregated as dollars, or measured directly by the needed number of endoscopies, treatments, etc., as estimated by the model. Numbers of complications and of treatment-related deaths can also be computed directly from these outputs, provided estimates of per-procedure complication rates are available.



[Readers Guide](#)
[Model Overview](#)
[Assumption Overview](#)
[Parameter Overview](#)
[Component Overview](#)
[Output Overview](#)
[Results Overview](#)
[Key References](#)



RESULTS OVERVIEW

SUMMARY

This document provides an overview of the results produced by EACMo.

RESULTS LIST



[Readers Guide](#)
[Model Overview](#)
[Assumption Overview](#)
[Parameter Overview](#)
[Component Overview](#)
[Output Overview](#)
[Results Overview](#)
[Key References](#)

Cytosponge Screening for Barrett's Esophagus

The Cytosponge is a noninvasive cell-sampling device that can identify Barrett's esophagus, a precursor to esophageal adenocarcinoma, in patients with GERD. In this analysis, done with the current version of EACMo and the UW-MISCAN model, it was found that first-line screening of patients with GERD with the Cytosponge is cost-effective.¹

Cost effectiveness of radiofrequency ablation for Barrett's esophagus

This analysis assessed effectiveness and cost-effectiveness of radiofrequency ablation (RFA) using a simple precursor to the current version of EACMo. It was found that RFA was cost-effective (compared to endoscopic surveillance) for patients with high grade dysplasia, might be cost-effective for low grade dysplasia, and might not be cost-effective for Barrett's with no dysplasia.²

In a later joint analysis with the FHCRC and UW-MISCAN modeling groups, it was found that all three models confirmed current guidelines endorsing RFA for patients with high grade dysplasia. The models diverged on low grade dysplasia eradication conclusions, highlighting the need to better understand the health state.³

Projections of esophageal cancer incidence and mortality

Calibrated natural history models were used to provide future projections of esophageal cancer incidence and mortality. This was a collaborative modeling exercise performed in conjunction with the FHCRC and UW-MISCAN modeling groups.⁴

The impact of obesity on the rise in esophageal adenocarcinoma incidence

Understanding the rise in EAC incidence is a critical goal of EACMo. This analysis used an early version of the model to measure the extent to which this rise could be attributed to the concurrent rise in obesity rates. It was found that obesity could account for only a small percentage of the increase.⁵

The prevalence of Barrett's esophagus in the US

Barrett's esophagus is a precursor to and risk factor for EAC. It's prevalence in the population is difficult to estimate, but has public health significance. This analysis used an early version of EACMo to estimate the true prevalence of BE at 5.6%, based on model fit to SEER incidence data.⁶

Development, calibration, and validation of a U.S. white male population-based simulation model of esophageal adenocarcinoma

Contains details on an early version of EACMo, and an analysis of aspirin chemoprevention.⁷



REFERENCES:

- ¹ Heberle, CR, Omidvari, AH, Ali, A, Kroep, S, Kong, CY, Inadomi, JM, Rubenstein, JH, Tramontano, AC, Dowling, EC, Hazelton, WD, Luebeck, EG, Lansdorp-Vogelaar, I, Hur, C "Cost Effectiveness of Screening Patients With Gastroesophageal Reflux Disease for Barrett's Esophagus With a Minimally Invasive Cell Sampling Device" in *Clin Gastroenterol Hepatol* 2017; 15: 9: 1397-1404
- ² Hur C, Choi SE, Rubenstein JH, Kong CY, Nishioka NS, Provenzale DT, Inadomi JM "The cost effectiveness of radiofrequency ablation for Barrett's esophagus" in *Gastroenterology* 2012;
- ³ Kroep, S, Heberle, CR, Curtius, K, Kong, CY, Lansdorp-Vogelaar, I, Ali, A, Wolf, WA, Shaheen, NJ, Spechler, SJ, Rubenstein, JH, Nishioka, NS, Meltzer, SJ, Hazelton, WD, van Ballegooijen, M, Tramontano, AC, Gazelle, GS, Luebeck, EG, Inadomi, JM, Hur, C "Radiofrequency Ablation of Barrett's Esophagus Reduces Esophageal Adenocarcinoma Incidence and Mortality in a Comparative Modeling Analysis" 2017; 15: 9: 1471-1474
- ⁴ Kong CY, Kroep S, Curtius K, Hazelton WD, Jeon J, Meza R, Heberle CR, Miller MC, Choi SE, Lansdorp-Vogelaar I, van Ballegooijen M, Feuer EJ, Inadomi JM, Hur C, Luebeck EG "Exploring the recent trend in esophageal adenocarcinoma incidence and mortality using comparative simulation modeling." in *Cancer Epidemiol Biomarkers Prev.* 2014; 23: 6: 997-1006
- ⁵ Kong CY, Nattinger KJ, Hayeck TJ, Omer ZB, Wang YC, Spechler SJ, McMahon PM, Gazelle GS, Hur C "The impact of obesity on the rise in esophageal adenocarcinoma incidence: estimates from a disease simulation model" in *Cancer Epidemiol Biomarkers Prev* 2011;
- ⁶ Hayeck TJ, Kong CY, Spechler SJ, Gazelle GS, Hur C "The prevalence of Barrett's esophagus in the US: estimates from a simulation model confirmed by SEER data" in *Dis Esophagus* 2010;
- ⁷ Hur C, Hayeck TJ, Yeh JM, Richards EM, Spechler SJ, Gazelle GS, Kong CY "Development, calibration, and validation of a U.S. white male population-based simulation model of esophageal adenocarcinoma" in *PLoS One* 2010;



KEY REFERENCES

- Hayeck TJ, Kong CY, Spechler SJ, Gazelle GS, Hur C** (2010) The prevalence of Barrett's esophagus in the US: estimates from a simulation model confirmed by SEER data in *Dis Esophagus*,
- Heberle, CR, Omidvari, AH, Ali, A, Kroep, S, Kong, CY, Inadomi, JM, Rubenstein, JH, Tramontano, AC, Dowling, EC, Hazelton, WD, Luebeck, EG, Lansdorp–Vogelaar, I, Hur, C** (2017) Cost Effectiveness of Screening Patients With Gastroesophageal Reflux Disease for Barrett's Esophagus With a Minimally Invasive Cell Sampling Device in *Clin Gastroenterol Hepatol* 15:9, p 1397–1404
- Hur C, Choi SE, Rubenstein JH, Kong CY, Nishioka NS, Provenzale DT, Inadomi JM** (2012) The cost effectiveness of radiofrequency ablation for Barrett's esophagus in *Gastroenterology*,
- Hur C, Hayeck TJ, Yeh JM, Richards EM, Spechler SJ, Gazelle GS, Kong CY** (2010) Development, calibration, and validation of a U.S. white male population–based simulation model of esophageal adenocarcinoma in *PLoS One*,
- Institute of Medicine** (2009) Initial National Priorities for Comparative Effectiveness Research,
- Kong CY, Nattinger KJ, Hayeck TJ, Omer ZB, Wang YC, Spechler SJ, McMahon PM, Gazelle GS, Hur C** (2011) The impact of obesity on the rise in esophageal adenocarcinoma incidence: estimates from a disease simulation model in *Cancer Epidemiol Biomarkers Prev*,
- Kong CY, Kroep S, Curtius K, Hazelton WD, Jeon J, Meza R, Heberle CR, Miller MC, Choi SE, Lansdorp–Vogelaar I, van Ballegooijen M, Feuer EJ, Inadomi JM, Hur C, Luebeck EG** (2014) Exploring the recent trend in esophageal adenocarcinoma incidence and mortality using comparative simulation modeling. in *Cancer Epidemiol Biomarkers Prev*. 23:6, p 997–1006
- Kroep, S, Heberle, CR, Curtius, K, Kong, CY, Lansdorp–Vogelaar, I, Ali, A, Wolf, WA, Shaheen, NJ, Spechler, SJ, Rubenstein, JH, Nishioka, NS, Meltzer, SJ, Hazelton, WD, van Ballegooijen, M, Tramontano, AC, Gazelle, GS, Luebeck, EG, Inadomi, JM, Hur, C** (2017) Radiofrequency Ablation of Barrett's Esophagus Reduces Esophageal Adenocarcinoma Incidence and Mortality in a Comparative Modeling Analysis 15:9, p 1471–1474
- Locke GR, 3rd, Talley NJ, Fett SL, Zinsmeister AR, Melton LJ, 3rd.** (1997) Prevalence and clinical spectrum of gastroesophageal reflux: a population–based study in Olmsted County, Minnesota. in *Gastroenterology* 112:5, p 1448–56
- Ries LAG, Melbert D, Krapcho M, Stinchcomb DG, Howlander N, et al.** (2008) SEER Cancer Statistics Review, 1975–2005,
- Shaheen NJ, Crosby MA, Bozynski EM, Sandler RS** (2000) Is there publication bias in the reporting of cancer risk in Barrett's esophagus? in *Gastroenterology* 119:2, p 333–8
- Williamson WA, Ellis FH Jr, Gibb SP, Shahian DM, Aretz HT, Heatley GJ, Watkins E Jr.** (1991) Barrett's esophagus. Prevalence and incidence of adenocarcinoma. in *Archives of Internal Medicine* 151:11, p 2212–6



FLEXKB DOCUMENT
Version: HI.001.01242019.73031
Document generated: 01/24/2019

ERASMUS/UNIVERSITY OF WASHINGTON



Readers Guide
Model Overview
Assumption Overview
Parameter Overview
Component Overview
Output Overview
Results Overview
Key References

Important note: This document will remain archived as a technical appendix for publications. New versions will be added periodically as model refinements and updates are completed. The most current version is available at <http://cisnet.cancer.gov/profiles>. The CISNET model profile topics are not necessarily meant to be read in sequential fashion, so the reader should feel free to skip around as their interests dictate.

We recommend you let your interests guide you through this document, using the navigation tree as a general guide to the content available.

The intent of this document is to provide the interested reader with insight into ongoing research. Model parameters, structure, and results contained herein should be considered representative but preliminary in nature.

We encourage interested readers to contact the contributors for further information.

Go directly to the: [Reader's Guide](#).



READERS GUIDE

CORE PROFILE DOCUMENTATION

These topics will provide an overview of the model without the burden of detail. Each can be read in about 5–10 minutes. Each contains links to more detailed information if required.

Model Purpose

This document describes the primary purpose of the model.

Model Overview

This document describes the primary aims and general purposes of this modeling effort.

Assumption Overview

An overview of the basic assumptions inherent in this model.

Parameter Overview

Describes the basic parameter set used to inform the model, more detailed information is available for each specific parameter.

Component Overview

A description of the basic computational building blocks (components) of the model.

Output Overview

Definitions and methodologies for the basic model outputs.

Results Overview

A guide to the results obtained from the model.

Key References

A list of references used in the development of the model.



MODEL PURPOSE

SUMMARY

This part describes the purpose(s) for which the Erasmus/UW model was developed.

PURPOSE

The Erasmus/UW model was constructed for multiple purposes. First, we intend to gain better insight into the natural history of esophagus adenocarcinoma (EAC), especially with regards to the process by which cancer develops from Barrett's esophagus (BE). Second, the model is used to identify the driving factors for the substantial increase in EAC incidence over the last several decades. The model is able to inform investigators which factors might inform plausible explanations for the period or birth cohort effects observed in the BE and EAC increases. Finally, the model is used in comparative effectiveness studies to calculate consequences of screening, surveillance and treatment strategies.



MODEL OVERVIEW

SUMMARY

The Erasmus/UW model is a semi-Markov microsimulation model and includes three components:

- demography
- natural history
- screening

It uses the Monte Carlo method to simulate all events in the program. Possible events are birth and death of a person, BE incidence, and transitions from one state of disease to another. The individual life histories are simulated in the demography component of the model. The natural history component of Erasmus/UW simulates the development of EAC in the population which can be interrupted by screening in the screening component of the model.

PURPOSE

The Erasmus/UW model was constructed for multiple purposes. See details in [Model Purpose](#).

BACKGROUND

The Erasmus/UW model is a semi-Markov microsimulation model, which is based on the Microsimulation SCreening ANalysis (MISCAN) models also available for prostate, breast, colon and lung cancers. The population is simulated at the individual level with each person evolving through discrete disease states. However, instead of modeling yearly transitions with associated transition probabilities, the Erasmus/UW model generates durations in states. With the assumption of an exponential distribution of the duration in each state, this way of simulating leads to the same results as a Markov model with yearly transition probabilities. The advantage of the Erasmus/UW model approach is that durations in a certain state are not required to be a discrete value (they can be continuous). The model uses the Monte Carlo method to simulate all events in the program. Possible events are birth and death of a person, BE incidence, and transitions from one disease state to another.

The basic structure of the Erasmus/UW is separated into three main components:

- demography
- natural history
- screening

MODEL DESCRIPTION

The basic structure of the Erasmus/UW model is presented in figure 1. The model first simulates the life histories of a large population of individuals from birth to death. After this, the natural history of the disease is modeled according to current knowledge on BE incidence and malignant progression. Depending on age, sex and baseline individual risk, short or long segment BE may develop in an individual, which over time may progress to low-grade dysplasia (LGD) and high-grade dysplasia (HGD). In a minority of patients, malignant cells can arise from HGD, transforming to localized EAC that can progress sequentially into regional and advanced EAC.

In every preclinical cancer stage, there is a probability of the cancer being diagnosed due to the development of symptoms. The cure rate and survival after diagnosis depend on the stage of cancer. Patients may die of other causes at any moment during their lifetime.

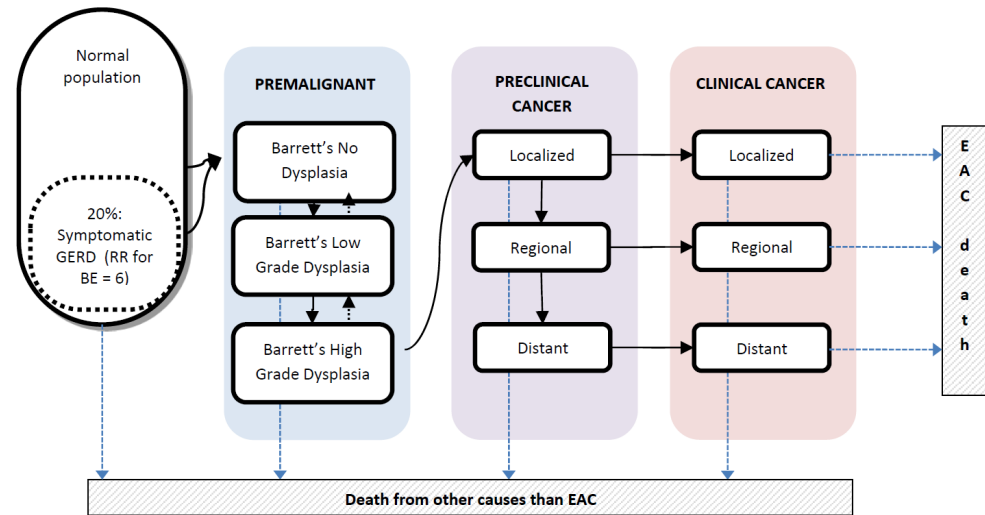


Figure 1. Erasmus/UW-EAC model

DEMOGRAPHY COMPONENT

The individual life histories are simulated in the demography component of the model. For each person, birth date and death date are simulated for causes other than EAC. The distribution of births and deaths can be adjusted to represent the simulated population.

NATURAL HISTORY COMPONENT

The natural history component of Erasmus/UW simulates the development of EAC in the population. We assume that EAC develops through precursor BE which starts in a phase without dysplasia, thereafter dysplasia can develop. Two stages of dysplasia are defined: low grade and high grade. From HGD, malignant cells can arise that can transform from this stage to preclinical localized EAC, which can sequentially progress into regional and distant preclinical EAC.

SCREENING COMPONENT

The development of EAC can be interrupted by screening and related palliative procedures. Screening can detect BE, the dysplasia states and preclinical cancers. BE and dysplasia can be removed using treatment. Usually, the cancers will be found in an earlier stage than with clinical diagnosis. In this way, screening reduces EAC incidence or EAC death.



ASSUMPTION OVERVIEW

SUMMARY

This part provides an overview of the main assumptions used in the Erasmus/UW model.

BACKGROUND

Several assumptions in the different parts of the model are considered to simplify the complex process of the disease progression and the interventions in a population. The assumptions are made in the following components;

- assumptions on demography
- assumptions on natural history
- assumptions on screening

ASSUMPTION LISTING

Demography Assumptions

These assumptions which focus on the demographic characteristics of the population are as follows:

- The life table differs in each cohort based on the birth year.
- Death from EAC cancer and other causes are considered independent from each other.

Natural History Assumptions

Natural history assumptions are related to the onset, progression, and response to treatment of EAC in the model. These assumptions are:

- Gastroesophageal Reflux Disease (GERD) prevalence is considered a fixed percentage of the population.
- BE development: in addition to development from no dysplasia to LGD and then HGD, BE patients could have also regression to the previous states, e. g. from HGD to LGD.
- BE incidence in the population is increasing until age 70.
- Types of BE: Long or short segment BE without dysplasia, with LGD or HGD.
- EAC cancer development: EAC can develop only through BE.
- Transition probabilities depend on the state of the disease.
- State durations depend on the state of the disease, e.g. patients with dysplasia have a shorter duration time than patients without dysplasia.
- Survival rates depend on the stage of cancer. It also depends on the year that they have got to that stage as the treatment modalities have been improved over the last decades which could improve the survival rates.

Screening Assumptions

These assumptions address the screening strategy parts in the model including attendance rate of the population, test characteristics and surveillance or treatment of the precancerous lesions as well. Assumptions are made on:



- Characteristics of screening tests: sensitivity of the screening test depends on the state of the disease.
- Attendance rate of the population is considered 100%.
- Impact of early detection and treatment of EAC which could improve the survival rate.
- Impact of detection of BE and treatment of dysplasia which prevent new EAC cases.
- Surveillance strategies after detection of BE patients are different according to the type of BE.



PARAMETER OVERVIEW

SUMMARY

This part provides an overview of the parameters used to quantify the Erasmus/UW model.

BACKGROUND

We have grouped the parameters in demographic, natural history, screening and output parameters.

PARAMETER LISTING OVERVIEW

Demography Parameters

1. number of birth cohorts
2. proportion of the population in each birth cohort
3. for each birth cohort parameters of its birth table
4. for each birth cohort the parameters of its life table

Natural history parameters

5. prevalence of GERD symptoms in the population
6. BE and EAC sequence states
7. parameters for the age specific distribution of onset of the first screen detectable state
8. parameters for the transition probability in each preclinical state
9. parameters for the duration distribution in each preclinical state
10. parameters for the time from a preclinical state to clinical detection
11. parameters for survival after clinical diagnosis by age at diagnosis, year of diagnosis, stage of disease and localization of the cancer
12. Parameters for proportion of low and high grade dysplasia in the BE population
13. Parameters for progression rate from each non-dysplastic (ND) BE, LGD and HGD to EAC

Screening test parameters

14. parameters for the dissemination of screening
15. the characteristics of screening test
16. parameters for survival after screen detected diagnosis
17. surveillance after screen-detected BE

Main natural history assumptions and results of the Erasmus/UW perfect and realistic model

Model parameter/value	Value in realistic model	Parameter characteristic *
Symptomatic GERD prevalence	20% of the total population	Fixed Input
BE from symptomatic GERD population	60% of total BE is from symptomatic GERD population	Fixed Input
BE prevalence age 60–64	1.4%	Optimized parameter
Percent of LGD in total BE at age 60–65	8.2%	Calibration target: 9.4%



- Readers Guide
- Model Overview
- Assumption Overview
- Parameter Overview
- Component Overview
- Output Overview
- Results Overview
- Key References

Percent of HGD in total BE at age 60–65	1.2%	Calibration target: 2.2%
Annual progression rate from diagnosed BE (ND+LGD) to clinical EAC	0.07%	Optimized parameter
Annual progression rate from diagnosed BE (ND+LGD) to clinical and detected EAC	0.18%	Calibration target: 0.18% in realistic model
Average sojourn time from preclinical cancer to clinical cancer, given transition	5.0	Calibration target: 4–5 year
Average time in BE to next transition	6.7	Optimized parameter
Average time in LGD to next transition	1.0	
Average time in HGD to next transition	1.1	
Regression transition probability		Optimized parameter
P(LGD to ND BE)	88%	
P(HGD to LGD)	15%	

* Fixed input: the parameter is defined as a fixed input of the model, Optimized parameter: the parameter is relaxed and is optimized during calibration of the model, the value is a result of the model; Calibration target: the model is calibrated to fit the fixed calibration targets as good as possible. Model is furthermore calibrated on the SEER–9 EAC incidence data from 2000–2009 for all males. GERD: Gastro–esophageal reflux disease; BE: Barrett’s esophagus; ND: No dysplasia; LGD: Low grade dysplasia; HGD: High grade dysplasia; EAC: Esophageal adenocarcinoma

The following sources were used to define these assumptions: ^{1,2,3,4,5,6,7,8,9,10,11,12,13,14}.

REFERENCES:

- Chiocca JC, Olmos JA, Salis GB, Soifer LO, Higa R, Marcolongo M. “Argentinean Gastro-Oesophageal Reflux Study G. Prevalence, clinical spectrum and atypical symptoms of gastro-oesophageal reflux in Argentina: a nationwide population-based study.” in *Alimentary Pharmacology & Therapeutics* 2005; 22: : 331-42
- Locke GR, 3rd, Talley NJ, Fett SL, Zinsmeister AR, Melton LJ. “Prevalence and clinical spectrum of gastroesophageal reflux: a population-based study in Olmsted County, Minnesota.” in *Gastroenterology* 1997; 112: : 1448-56
- Locke GR, 3rd, Talley NJ, Fett SL, Zinsmeister AR, Melton LJ. “Risk factors associated with symptoms of gastroesophageal reflux.” in *American Journal of Medicine* 1999; 106: : 642-9
- Mohammed I, Cherkas LF, Riley SA, Spector TD, Trudgill NJ. “Genetic influences in gastro-oesophageal reflux disease: a twin study.” in *Gut* 2003; 52: : 1085-9
- Ronkainen J, Aro P, Storskrubb T, Johansson SE, Lind T, Bolling-Sternevald E, Vieth M, Stolte M, Talley NJ, Agreus L. “Prevalence of Barrett’s esophagus in the general population: an endoscopic study.” in *Gastroenterology*. 2005; 129: : 1825-31
- Gruppo Operativo per lo Studio delle Precancerosi dell’Esofago (GOSPE). “Barrett’s esophagus: epidemiological and clinical results of a multicentric survey.” in *International Journal of Cancer* 1991; 48: 3: 364-8
- Guanrei Y, Songliang Q, He H, Guizen F. “Natural history of early esophageal squamous carcinoma and early adenocarcinoma of the gastric cardia in the People’s Republic of China.” in *Endoscopy* 1988; 20: : 95-8
- Provenzale D, Kemp JA, Arora S, Wong JB. “A guide for surveillance of patients with Barrett’s esophagus.” in *The American Journal of Gastroenterology* 1994; 89: : 670-80
- Shaheen NJ, Crosby MA, Bozyski EM, Sandler RS. “Is there publication bias in the reporting of cancer risk in Barrett’s esophagus?” in *Gastroenterology*. 2000; 119: : 333-8

- 10 Desai TK, Krishnan K, Samala N, Singh J, Cluley J, Perla S, Howden CW. "The incidence of oesophageal adenocarcinoma in non-dysplastic Barrett's oesophagus: a meta-analysis." in Gut 2012; 61: : 970-6
- 11 Yousef F, Cardwell C, Cantwell MM, Galway K, Johnston BT, Murray L. "The incidence of esophageal cancer and high-grade dysplasia in Barrett's esophagus: a systematic review and meta-analysis." in American Journal of Epidemiology 2008; 163: : 237-49
- 12 Hvid-Jensen F, Pedersen L, Drewes AM, Sorensen HT, Funch-Jensen P. "Incidence of adenocarcinoma among patients with Barrett's esophagus." in The New England Journal of Medicine 2011; 365: : 1375-83
- 13 de Jonge PJ, Steyerberg EW, Kuipers EJ, Honkoop P, Wolters LM, Kerkhof M, van Dekken H, Siersema PD. "Risk factors for the development of esophageal adenocarcinoma in Barrett's esophagus." in The American Journal of Gastroenterology 2006; 101: : 1421-9
- 14 Bhat S, Coleman HG, Yousef F, Johnston BT, Mc Manus DT, Gavin AT, Murray LJ. "Risk of malignant progression in Barrett's esophagus patients: results from a large population-based study." in Journal of the National Cancer Institute. 2011; 103: : 1049-57

COMPONENT OVERVIEW

SUMMARY

This part describes the main components of the Erasmus/UW model.

OVERVIEW

As described in the Model overview, Erasmus/UW model includes three components: demography, natural history and screening.

COMPONENT LISTING

Demography Component

The individual life histories are simulated in the demography component of the model. For each person, a birth date and death date is simulated for other causes than EAC. The demography parameters are birth table parameter and life table parameters.

Natural history Component

The Natural History component of Erasmus/UW simulates the development of EAC in the population. We assume that EAC develops through precursor long or short-segment BE. A personal risk index is generated for each individual in the simulated population. Figure 2 shows the modeling natural history with life history.

A minority of the population has symptomatic GERD, giving them a higher risk of developing BE during their lifetime. The development of BE (ND) is generated according to this personal risk index and an age-specific incidence of onset. The sequence from the onset of BE to EAC diagnosis is continued by sojourn times between the different states. BE starts in a phase without dysplasia, thereafter dysplasia can develop. Two stages of dysplasia are defined: LGD and HGD. From HGD, malignant cells can arise that can transform from this stage to preclinical localized EAC, which can sequentially progress into regional and distant preclinical EAC. There is a possibility that regression from HGD to LGD and from LGD to ND occurs. The probability to regress or progress is dependent on a transition matrix and is therefore also influenced by the sojourn time. In each of these three preclinical cancer stages, there is a probability of the cancer being diagnosed. The sojourn times between these described stages are exponentially distributed and in some cases (BE-ND, BE-LGD and BE-HGD) are age-dependent. Because most sojourn times extend beyond the demography-generated age of death from other causes, only a small proportion of the population develop EAC from BE. The survival after clinical diagnosis depends on the cancer stage and the year of diagnosis.

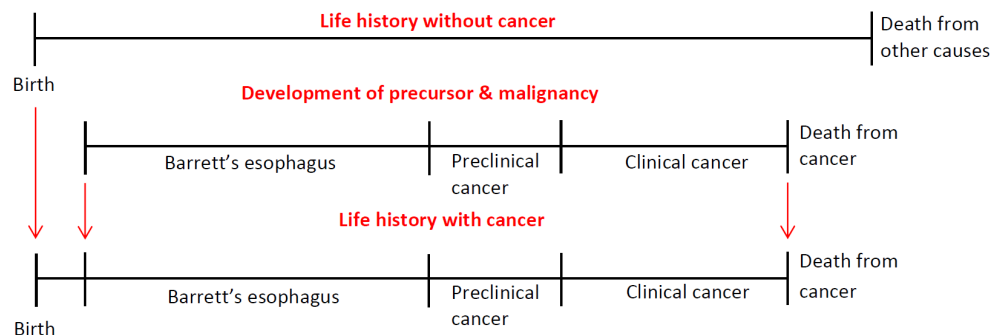


Figure 2. Modeling natural history with life history

Erasmus/UW distinguishes the following states of the disease process:

1. normal, no known disease

Preclinical

2. non-dysplastic short segment BE
3. short segment BE with Low-grade dysplasia
4. short segment BE with High-grade dysplasia
5. non-dysplastic Long segment BE
6. long segment BE with Low-grade dysplasia
7. long segment BE with High-grade dysplasia

Invasive

8. preclinical cancer localized
9. preclinical cancer regional
10. preclinical cancer distant

Clinical

11. clinical cancer localized
12. clinical cancer regional
13. clinical cancer distant

Screening Component

The screening component is simultaneously run with the natural history component. The development of EAC can be interrupted by screening. Screening can detect BE, the dysplasia states and preclinical cancers. Patients with BE and dysplasia could be kept under surveillance or BE and dysplasia can be removed using treatment. In this situation, usually, the cancers will be found in an earlier stage than with clinical diagnosis. See Figure 3 for modeling screening and treatment interventions into life history.

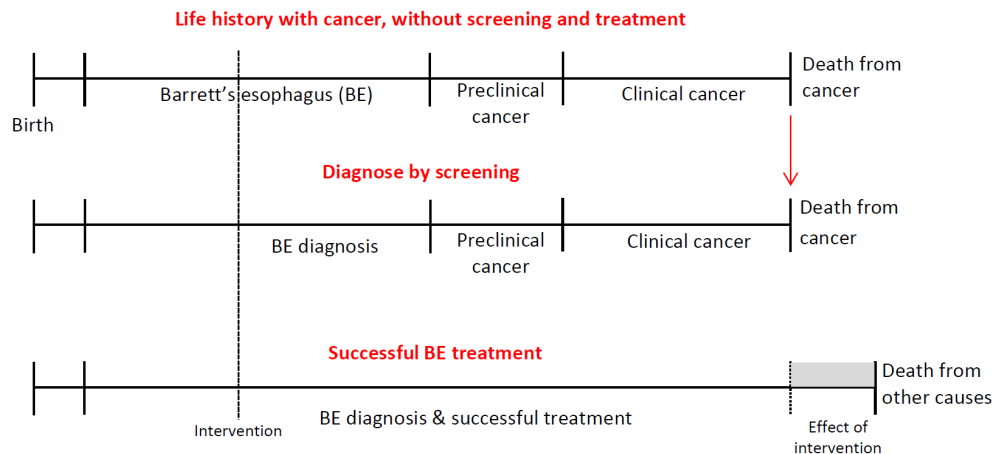


Figure 3. Modeling screening and treatment interventions



OUTPUT OVERVIEW

SUMMARY

This part provides overview of the outputs generated by the Erasmus/UW model.

OUTPUT LISTING

The outputs are generated by Erasmus/UW model include:

1. incidence counts of each disease state by calendar year
2. mean prevalence of each disease state in five year age groups
3. number of invitations for screen tests, and surveillance for each year
4. number of positive and negative test results per disease state and per year
5. number of specific deaths and non-specific deaths
6. total number of life years and life years lost due to cancer
7. number of life years gained due to screening by year of screening
8. total number of life years in surveillance
9. total number of life years with initial therapy after screen-detected or clinical cancer for each state
10. total number of life years with continuous care after screen-detected or clinical cancer for each state
11. total number of life years with terminal care before death from other causes
12. total number of life years with terminal care before death from EAC

RESULTS OVERVIEW

SUMMARY

This part describes the results obtained from the Erasmus/UW model.

OVERVIEW

The Erasmus/UW model has been applied to inform policies with regards to screening of the population, surveillance and management of patients with GERD and BE to prevent EAC. The result part describes the studies which have used Erasmus/UW model.

RESULTS LIST

Estimation of future U.S. EAC incidence

The Erasmus/UW model was calibrated to clinical and epidemiologic data including EAC incidence from the Surveillance, Epidemiology, and End Results (SEER 9) registry from 1975–2010 to project EAC incidence and mortality to year 2030. The results obtained from Erasmus/UW model were compared with two other independently developed models (FHCRC and MGH) as well.

Importantly, all three models identified birth cohort trends affecting cancer progression as a major driver of the observed increases in EAC incidence and mortality. All models predict that incidence and mortality rates will continue to increase until 2030 but with a plateauing trend for recent male cohorts. The predicted ranges of incidence and mortality rates (cases per 100,000 person-years) in 2030 are 8.4–10.1 and 5.4–7.4 respectively for males, and 1.3–1.8 and 0.9–1.2 for females. Figure 4 shows the EAC incidence rates by 10 year birth cohorts for all males. The cohort born in 1959 would be 71 years old in calendar year 2030. The details are described in Kong CY, et al. 2014 paper.¹

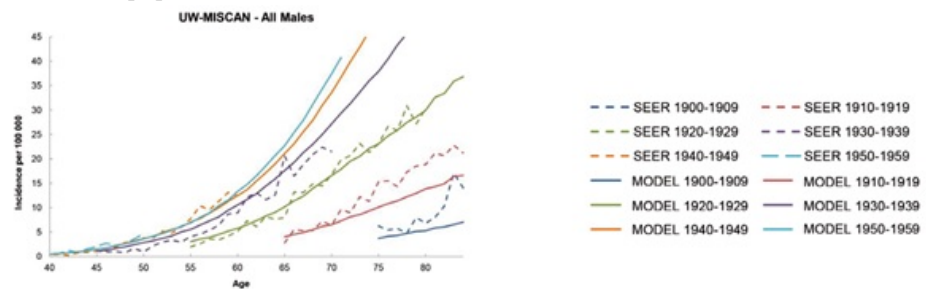


Figure 4. The EAC incidence rates by 10 year birth cohorts for all males

Estimation of the rate of progression from BE to EAC

The Erasmus/UW model was used to reconcile published data and more accurately estimate the incidence of EAC among people with BE. The calibration to the population-based study, including realistic surveillance, resulted in an annual progression rate of 0.19% for BE to EAC with a 5-year follow-up. The same disease model predicted a 0.36% annual rate of progression in studies with a prospective design. Therefore, in the first 5 years after diagnosis, the rate of progression from BE to EAC is likely to more closely approximate the lower estimates reported from population-based studies than the higher estimates reported from prospective studies, in which EAC is detected by surveillance.

The result of this study could be used by clinicians to explain to patients their risk if no

action is taken, and then discuss the risks and benefits of surveillance. You can find details in Kroep S, et al. 2015.²

As the previous study showed that estimates for the annual progression rate from BE to EAC vary widely, it was also quantified that how this uncertainty impacts the estimates of effectiveness and efficiency of screening and treatment for EAC. This uncertainty could seriously hamper decision-making regarding the implementation of BE screening and treatment interventions. The details are described in Kroep S, et al. 2015 paper.³

Estimation of the impact of endoscopic eradication for BE on EAC incidence and mortality

New techniques for the endoscopic eradication of the EAC precursor BE such as radiofrequency ablation (RFA) is utilized to prevent progression to EAC. The efficacy and durability of endoscopic eradication are reported, but the long-term impact of eradication and recurrent disease on EAC incidence and overall mortality reduction has not been analyzed with comprehensive and robust simulation models using this recently updated clinical data. The Erasmus/UW model was used to analyze the impact of RFA for the endoscopic eradication of BE with or without dysplasia on EAC incidence and mortality. The results obtained from the Erasmus/UW model were compared with other two aforementioned models as well.

The models showed that a strategy to endoscopically eradicate BE with high-grade dysplasia will decrease EAC incidence by 50% (range 44%–58%) and EAC mortality by 46% (41%–53%). The results indicated that RFA is an effective means of reducing EAC incidence and mortality. The benefit is predicted to be achieved in all patients with BE; however, the efficiency of eradication is substantially reduced if patients with LGD and no dysplasia are treated, and substantially more healthcare resources are required to avert a cancer death in these settings. Figure 5 shows the mortality reduction compared to the total number of treatments per model and strategy.⁴

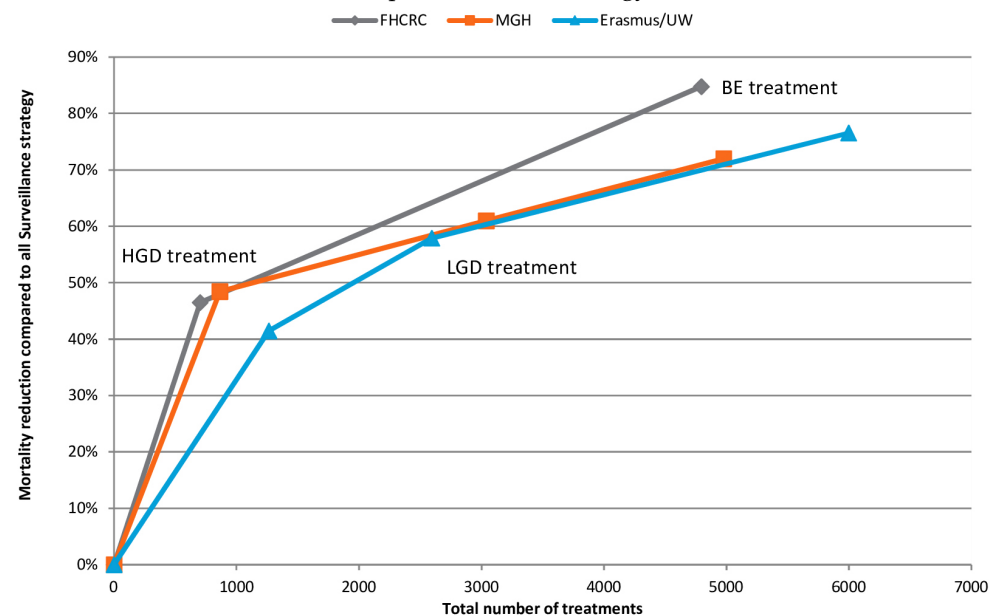


Figure 5. Mortality reduction compared to the total number of treatments per model and strategy. BE: Barrett’s esophagus, EAC: esophageal adenocarcinoma, Strategies: HGD: Endoscopic ablative therapy for HGD diagnosed patients strategy; LGD: Endoscopic ablative therapy for dysplasia diagnosed patients strategy; BE: Endoscopic ablative therapy for all BE diagnosed patients strategy.

Analyzing the cost-effectiveness of Cytosponge for screening patients at high risk of developing EAC or BE

The Erasmus/UW and MGH models were used to analyze the cost-effectiveness of Cytosponge as a first-line screening method with endoscopic confirmation for positive results in patients at high risk of developing EAC or BE. The models suggested that initial Cytosponge with endoscopic confirmation would be a cost-effective screening strategy for patients with GERD symptoms. The greatest benefit was achieved by endoscopic screening, but with an unfavorable marginal cost. Figure 6 shows more details regarding cost and QALY gained per strategy and the model.⁵

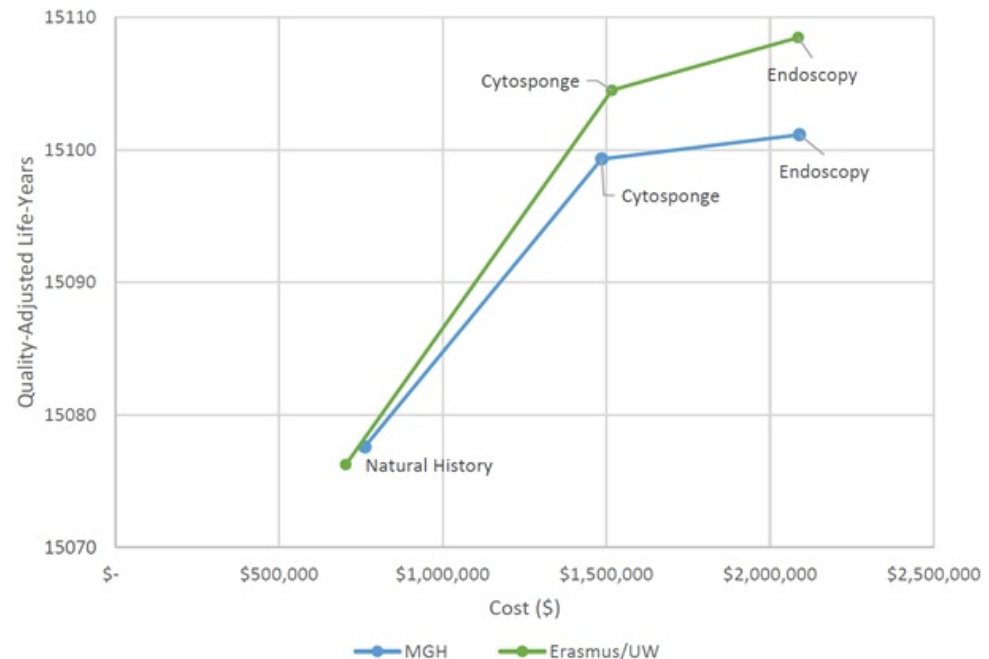


Figure 6. Cost/benefit curves for the MGH (blue) and Erasmus/UW (green) models.

REFERENCES:

- 1 Kong CY, Kroep S, Curtius K, Hazelton WD, Jeon J, Meza R, Heberle CR, Miller MC, Choi SE, Lansdorp-Vogelaar I, van Ballegooijen M, Feuer EJ, Inadomi JM, Hur C, Luebeck EG "Exploring the recent trend in esophageal adenocarcinoma incidence and mortality using comparative simulation modeling" in *Cancer Epidemiology, Biomarkers & Prevention* 2014; 23: : 997-1006
- 2 Kroep S1, Lansdorp-Vogelaar I, Rubenstein JH, de Koning HJ, Meester R, Inadomi JM, van Ballegooijen M "An Accurate Cancer Incidence in Barrett's Esophagus: A Best Estimate Using Published Data and Modeling" in *Gastroenterology* 2015; 149: 3: 577-85.e4
- 3 Kroep S2, Lansdorp-Vogelaar I, van der Steen A, Inadomi JM, van Ballegooijen M. "The Impact of Uncertainty in Barrett's Esophagus Progression Rates on Hypothetical Screening and Treatment Decisions" in *Medical Decision Making* 2015; 35: 6: 726-33
- 4 Kroep S, Heberle CR, Curtius K, Kong CY, Lansdorp-Vogelaar I, Ali A, Wolf WA, Shaheen NJ, Spechler SJ, Rubenstein JH, Nishioka NS, Meltzer SJ, Hazelton



Erasmus/UW
Results Overview
References:

WD, van Ballegooijen M, Tramontano AC, Gazelle GS, Luebeck EG, Inadomi JM, Hur C "Radiofrequency Ablation of Barrett's Esophagus Reduces Esophageal Adenocarcinoma Incidence and Mortality in a Comparative Modeling Analysis" in *Clinical Gastroenterology and Hepatology* 2017; 15: 9: 1471-1474

⁵ Heberle CR, Omidvari AH, Ali A, Kroep S, Kong CY, Inadomi JM, Rubenstein JH, Tramontano AC, Dowling EC, Hazelton WD, Luebeck EG, Lansdorp-Vogelaar I, Hur C. "Cost Effectiveness of Screening Patients With Gastroesophageal Reflux Disease for Barrett's Esophagus With a Minimally Invasive Cell Sampling Device" in *Clinical Gastroenterology and Hepatology* 2017; 15: 9: 1397-1404

KEY REFERENCES

- Bhat S, Coleman HG, Yousef F, Johnston BT, Mc Manus DT, Gavin AT, Murray LJ.** (2011) Risk of malignant progression in Barrett's esophagus patients: results from a large population-based study. in *Journal of the National Cancer Institute*. 103, p 1049–57
- Chiocca JC, Olmos JA, Salis GB, Soifer LO, Higa R, Marcolongo M.** (2005) Argentinean Gastro-Oesophageal Reflux Study G. Prevalence, clinical spectrum and atypical symptoms of gastro-oesophageal reflux in Argentina: a nationwide population-based study. in *Alimentary Pharmacology & Therapeutics* 22, p 331–42
- Desai TK, Krishnan K, Samala N, Singh J, Cluley J, Perla S, Howden CW.** (2012) The incidence of oesophageal adenocarcinoma in non-dysplastic Barrett's oesophagus: a meta-analysis. in *Gut* 61, p 970–6
- Gruppo Operativo per lo Studio delle Precancerosi dell'Esofago (GOSPE).** (1991) Barrett's esophagus: epidemiological and clinical results of a multicentric survey. in *International Journal of Cancer* 48:3, p 364–8
- Guanrei Y, Songliang Q, He H, Guizen F.** (1988) Natural history of early esophageal squamous carcinoma and early adenocarcinoma of the gastric cardia in the People's Republic of China. in *Endoscopy* 20, p 95–8
- Heberle CR, Omidvari AH, Ali A, Kroep S, Kong CY, Inadomi JM, Rubenstein JH, Tramontano AC, Dowling EC, Hazelton WD, Luebeck EG, Lansdorp-Vogelaar I, Hur C.** (2017) Cost Effectiveness of Screening Patients With Gastroesophageal Reflux Disease for Barrett's Esophagus With a Minimally Invasive Cell Sampling Device in *Clinical Gastroenterology and Hepatology* 15:9, p 1397–1404
- Hvid-Jensen F, Pedersen L, Drewes AM, Sorensen HT, Funch-Jensen P.** (2011) Incidence of adenocarcinoma among patients with Barrett's esophagus. in *The New England Journal of Medicine* 365, p 1375–83
- Kong CY, Kroep S, Curtius K, Hazelton WD, Jeon J, Meza R, Heberle CR, Miller MC, Choi SE, Lansdorp-Vogelaar I, van Ballegooijen M, Feuer EJ, Inadomi JM, Hur C, Luebeck EG** (2014) Exploring the recent trend in esophageal adenocarcinoma incidence and mortality using comparative simulation modeling in *Cancer Epidemiology, Biomarkers & Prevention* 23, p 997–1006
- Kroep S, Heberle CR, Curtius K, Kong CY, Lansdorp-Vogelaar I, Ali A, Wolf WA, Shaheen NJ, Spechler SJ, Rubenstein JH, Nishioka NS, Meltzer SJ, Hazelton WD, van Ballegooijen M, Tramontano AC, Gazelle GS, Luebeck EG, Inadomi JM, Hur C** (2017) Radiofrequency Ablation of Barrett's Esophagus Reduces Esophageal Adenocarcinoma Incidence and Mortality in a Comparative Modeling Analysis in *Clinical Gastroenterology and Hepatology* 15:9, p 1471–1474
- Kroep S1, Lansdorp-Vogelaar I, Rubenstein JH, de Koning HJ, Meester R, Inadomi JM, van Ballegooijen M** (2015) An Accurate Cancer Incidence in Barrett's Esophagus: A Best Estimate Using Published Data and Modeling in *Gastroenterology* 149:3, p 577–85.e4
- Kroep S2, Lansdorp-Vogelaar I, van der Steen A, Inadomi JM, van Ballegooijen M.** (2015) The Impact of Uncertainty in Barrett's Esophagus Progression Rates on Hypothetical Screening and Treatment Decisions in *Medical Decision Making* 35:6, p 726–33
- Locke GR, 3rd, Talley NJ, Fett SL, Zinsmeister AR, Melton LJ.** (1999) Risk factors associated with symptoms of gastroesophageal reflux. in *American Journal of Medicine* 106, p 642–9

- Locke GR, 3rd, Talley NJ, Fett SL, Zinsmeister AR, Melton LJ.** (1997) Prevalence and clinical spectrum of gastroesophageal reflux: a population-based study in Olmsted County, Minnesota. in *Gastroenterology* 112, p 1448–56
- Mohammed I, Cherkas LF, Riley SA, Spector TD, Trudgill NJ.** (2003) Genetic influences in gastro-oesophageal reflux disease: a twin study. in *Gut* 52, p 1085–9
- Provenzale D, Kemp JA, Arora S, Wong JB.** (1994) A guide for surveillance of patients with Barrett's esophagus. in *The American Journal of Gastroenterology* 89, p 670–80
- Ronkainen J, Aro P, Storskrubb T, Johansson SE, Lind T, Bolling-Sternevald E, Vieth M, Stolte M, Talley NJ, Agreus L.** (2005) Prevalence of Barrett's esophagus in the general population: an endoscopic study. in *Gastroenterology*. 129, p 1825–31
- Shaheen NJ, Crosby MA, Bozymski EM, Sandler RS.** (2000) Is there publication bias in the reporting of cancer risk in Barrett's esophagus? in *Gastroenterology*. 119, p 333–8
- Yousef F, Cardwell C, Cantwell MM, Galway K, Johnston BT, Murray L.** (2008) The incidence of esophageal cancer and high-grade dysplasia in Barrett's esophagus: a systematic review and meta-analysis. in *American Journal of Epidemiology* 163, p 237–49
- de Jonge PJ, Steyerberg EW, Kuipers EJ, Honkoop P, Wolters LM, Kerkhof M, van Dekken H, Siersema PD.** (2006) Risk factors for the development of esophageal adenocarcinoma in Barrett's esophagus. in *The American Journal of Gastroenterology* 101, p 1421–9
-



FLEXKB DOCUMENT
Version: HI.001.01242019.73031
Document generated: 01/24/2019



[Readers Guide](#)
[Model Overview](#)
[Assumption Overview](#)
[Parameter Overview](#)
[Component Overview](#)
[Output Overview](#)
[Results Overview](#)
[Key References](#)

FRED HUTCHINSON CANCER RESEARCH CENTER

Important note: This document will remain archived as a technical appendix for publications. New versions will be added periodically as model refinements and updates are completed. The most current version is available at <http://cisnet.cancer.gov/profiles>. The CISNET model profile topics are not necessarily meant to be read in sequential fashion, so the reader should feel free to skip around as their interests dictate.

We recommend you let your interests guide you through this document, using the navigation tree as a general guide to the content available.

The intent of this document is to provide the interested reader with insight into ongoing research. Model parameters, structure, and results contained herein should be considered representative but preliminary in nature.

We encourage interested readers to contact the contributors for further information.

Go directly to the: [Reader's Guide](#).



READERS GUIDE

CORE PROFILE DOCUMENTATION

These topics will provide an overview of the model without the burden of detail. Each can be read in about 5–10 minutes. Each contains links to more detailed information if required.

Model Purpose

This document describes the primary purpose of the model.

Model Overview

This document describes the primary aims and general purposes of this modeling effort.

Assumption Overview

An overview of the basic assumptions inherent in this model.

Parameter Overview

Describes the basic parameter set used to inform the model, more detailed information is available for each specific parameter.

Component Overview

A description of the basic computational building blocks (components) of the model.

Output Overview

Definitions and methodologies for the basic model outputs.

Results Overview

A guide to the results obtained from the model.

Key References

A list of references used in the development of the model.



MODEL PURPOSE

SUMMARY

This document provides an overview of the Fred Hutchinson Cancer Research Center (FHCRC) multistage clonal expansion for esophageal adenocarcinoma (MSCE-EAC) model with multiple scales, including the cell, crypt, clonal patch, tissue [normal, Barrett's esophagus (BE), high grade dysplasia (HGD), and esophageal adenocarcinoma (EAC)], individual, and population levels. The model combines an age-dependent gastroesophageal reflux disease (GERD) component with multistage cell kinetic rates that depend on birth cohort to fit US EAC incidence data. Both likelihood-based and detailed multiscale spatial simulation methods are used for analysis and prediction of EAC trends and effects of alternative screening and treatment protocols.

PURPOSE

The purpose of the MSCE-EAC model is to serve as an effective tool for evaluating EAC trends in the US population and the impact of possible interventions on modifying future cancer trends. The model combines rigorous likelihood-based estimation of cell kinetic rates that drive the cancer process with detailed spatial simulation of the growth and extinction of premalignant and malignant clones to evaluate the sensitivities of different biopsy and advanced endoscopic imaging protocols and the potential benefits and harms of radio-frequency ablation or other treatment methods.



MODEL OVERVIEW

SUMMARY

The MSCE–EAC model provides a mathematical and computational framework for multiscale modeling of the natural history of progression from normal esophageal squamous epithelium to esophageal adenocarcinoma (EAC), and the impact of alternative protocols for biopsy, imaging, and treatment.

PURPOSE

The purpose of the MSCE–EAC model is to provide insight into the biology and natural history of progression and detection of EAC over many length and time scales, beginning with models of fundamental processes represented at the cellular level.

The development of BE is recognized as an early step in progression to EAC, with an enhanced risk for BE among individuals with gastroesophageal reflux disease (GERD) symptoms. The model represents age–dependent development of weekly or more frequent GERD symptoms, with transitions from both GERD and non–GERD pathways to develop BE, two additional mutations or epigenetic changes for the initiation of HGD, with clonal expansion of cells comprising HGD, malignant transformation, and a more rapid clonal expansion process for EAC.

GERD incidence data were utilized to calibrate the model for age–dependent GERD prevalence, and Surveillance Epidemiology and End Results (SEER) incidence data were used for likelihood–based calibration of the remaining parameters of the multiscale EAC progression model.

EAC incidence has increased approximately six–fold in the US since 1975, as reflected in SEER data.¹ These temporal trends were modeled by systematically applying flexible period and cohort trends to the biological parameters of the MSEAC model, and using likelihood methods for model comparison and selection of the best model fit to SEER incidence.

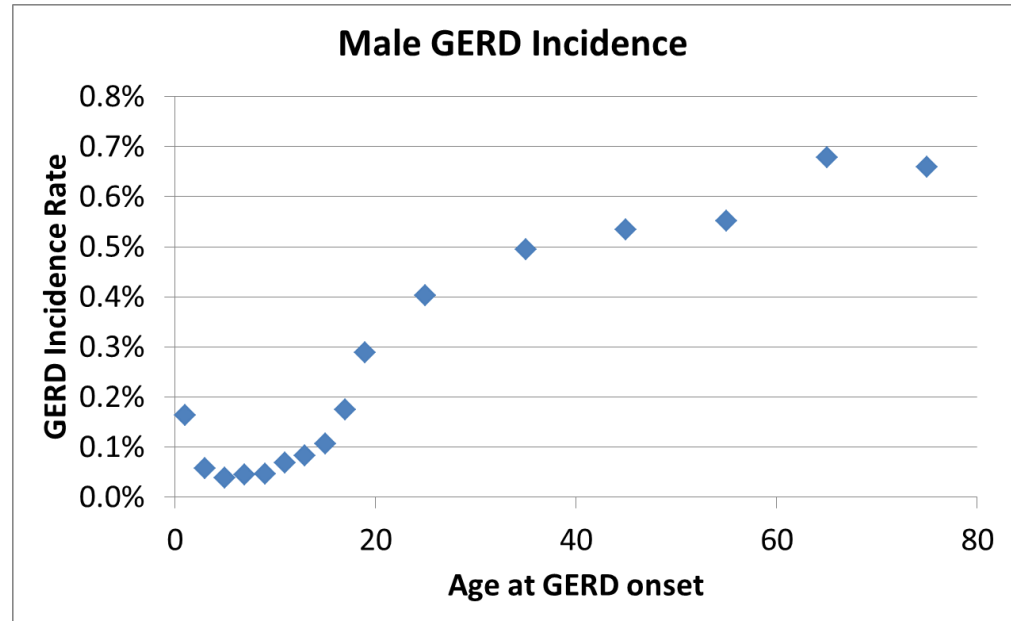
To identify which biological parameters may be influenced by temporal trends, we compared alternative models with period and/or cohort effects influencing GERD development, the transition rate to BE, early mutation steps, growth of premalignant lesions, malignant transformation, and clonal growth of the tumor. The best model fit includes a sigmoidal (birth) cohort trend on both premalignant and malignant clonal expansion (see [Results Overview](#)).

Spatial simulations of the growth of premalignant clones (identified with HGD) and malignant tumors are mapped to represent two–dimensional localization and growth on the BE segment of the esophageal surface (represented as a torus).

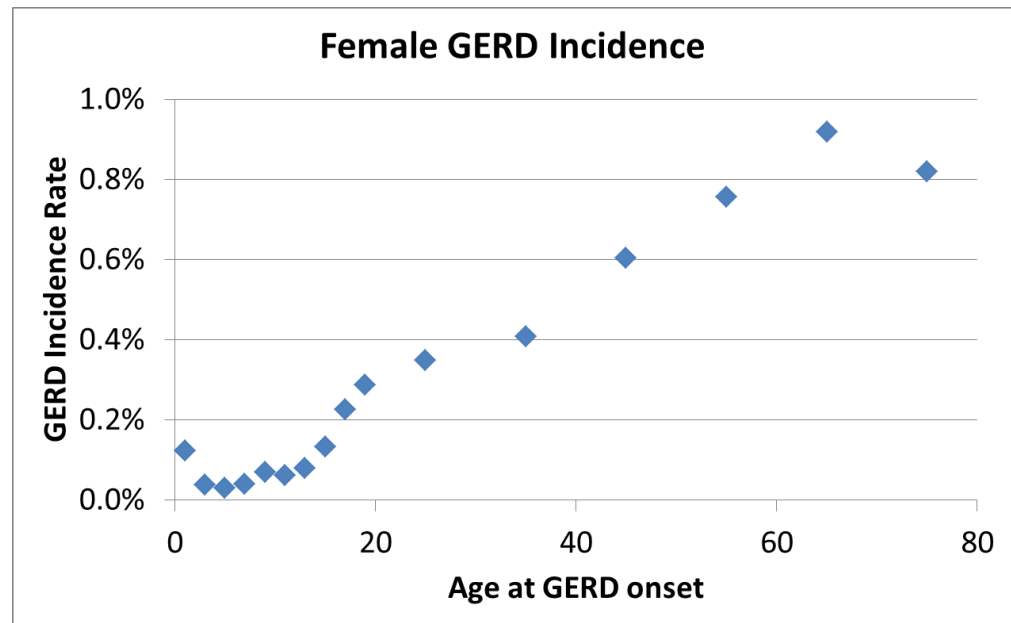
This spatial modeling component of the MSEAC model allows analysis of the probability for biopsy sampling of HGD and preclinical EAC during screening, along with symptomatic cancer detection. This framework is inherently 'multiscale' in that it bridges the cellular scale with the population scale, allowing us to model physically the process of endoscopic screening of BE patients for the presence of premalignant and preclinical malignant lesions prior to the appearance of cancer symptoms and/or a cancer diagnosis.

BACKGROUND

A clinically important component of the MSCE–EAC model is an underlying gender and age–specific model of GERD prevalence, which is generally believed to increase the relative risk for BE. Calibration of the GERD prevalence model utilized data from incident GERD cases in a cohort of 1700 children and adolescents in the Health Improvement Network (THIN) UK primary care database between 2000–2005,² and case–control data on adults with a first diagnosis of GERD in the UK General Practice Research Database (GPRD), including 7451 cases and 10,000 controls.³



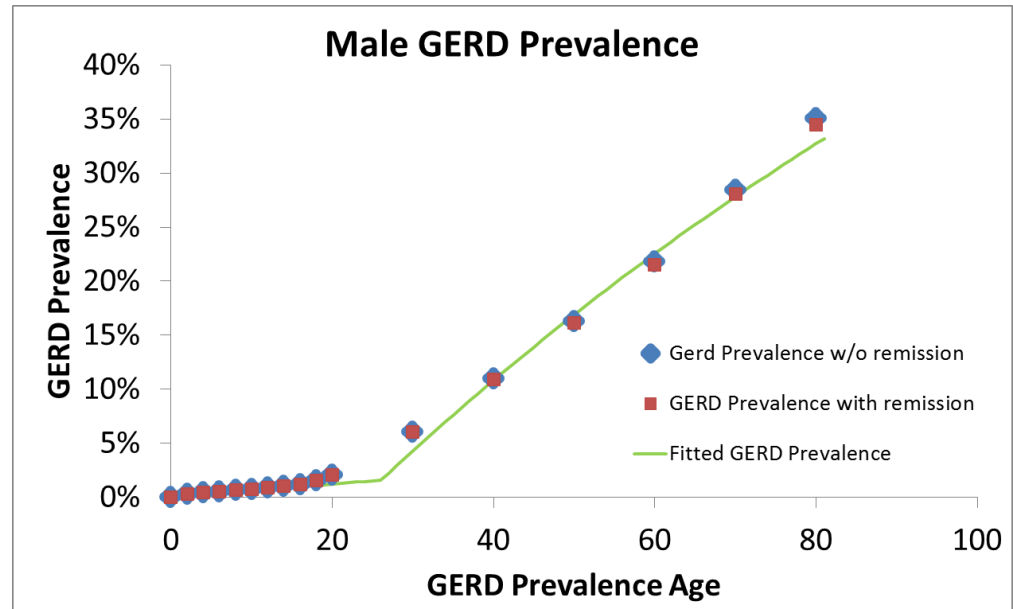
Data from Ruigomez, et al. (1,2)



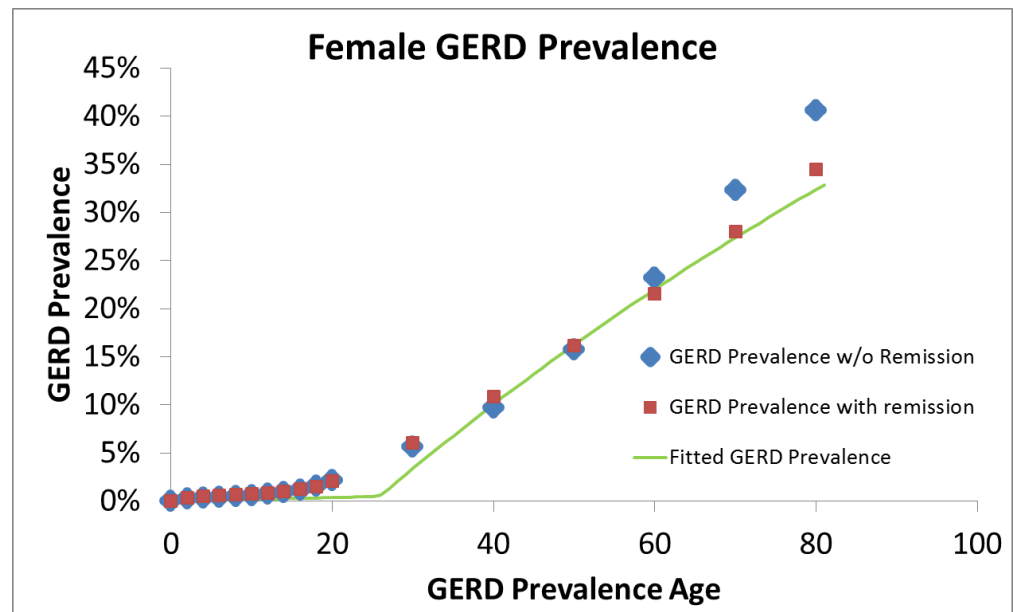
Data from Ruigomez, et al. (1,2)

GERD was defined as heartburn and/or regurgitation experienced at least weekly in these studies.^{2,3} Using this definition, we develop male and female GERD models with GERD prevalence increasing in accordance with the data for age–specific GERD

incidence.^{2,3} However, the models also include a parameter representing reversion rates of GERD symptoms, allowing us to fit age-adjusted GERD prevalence between ages 40 to 85 to an approximate target of 20%, consistent with population-based studies of GERD prevalence.^{4,5,6,7} We then use maximum likelihood methods to fit the data-driven models above and generate simpler 3-parameter gender and age-specific GERD prevalence models that represents an effective childhood/young adult transition rate to GERD, a transition age, and an effective older adult transition rate to GERD. (See green lines in Figures below).



Male GERD prevalence model



Female GERD prevalence model

Epidemiological studies indicate that most individuals with GERD do not develop BE, but that GERD is a significant risk factor for BE but with differing estimates of relative risk (RR) for BE given GERD ranging between 2–15%, and also depending on BE segment length, frequency of GERD symptoms and other factors.^{8,9} A recent

meta-analysis of 14 studies found an odds-ratio of at-least weekly GERD in relation to long segment BE of 4.92, CI=(2.01-12.0), and no association with short segment BE.⁹ Another recent meta-analysis of 5 studies on the association of GERD with EAC found an odds ratio of 4.92, CI= (3.92, 6.22).¹⁰

The model fits to SEER data allow prediction of the background transition rate to BE, and thus BE prevalence is predicted by including GERD and non-GERD pathways, with predictions of 1.5-5% BE prevalence for males for ages ranging between 40 and 85, and between 0.5-1% for females. Population estimates of BE prevalence differ widely,¹¹ but given this uncertainty, the model predictions appear generally consistent with the range of estimates in the studies.

SEER EAC incidence has increased roughly six-fold since 1975.^{1,12} To identify biological parameters that may be influenced by temporal trends, we compared alternative models with period and/or cohort effects influencing GERD development, the transition rate to BE, early mutation steps, growth of premalignant lesions, malignant transformation, and clonal growth of the tumor.

MODEL DESCRIPTION

The development of BE is recognized as an early step in progression to EAC, with an enhanced risk for BE among individuals with gastroesophageal reflux disease (GERD) symptoms. The model represents age-dependent development of weekly or more frequent GERD symptoms, with transitions from both GERD and non-GERD pathways to develop BE, two additional mutations or epigenetic changes for the initiation of HGD, with clonal expansion of cells comprising HGD, malignant transformation, and a more rapid clonal expansion process for EAC. The transition rate ν from normal to BE includes a baseline rate ν_0 for individuals without GERD and a faster rate for individuals with GERD modeled as $\nu_0 * RR$, where RR is the relative risk for BE given GERD. (Calibration of models for GERD and BE prevalences is discussed below).

Age-dependent model of prevalence for GERD and Barrett's esophagus

Let p_G be the probability of GERD at age t , with $p_G(t) = 1 - \exp[-r_1 \min(r_3, t) - r_2 \max(0, t - r_3)]$ being a three-parameter function that we fit to GERD incidence data^{2,3} and age-adjusted GERD prevalence,^{4,5,6,7} as described in the Background section.

We model the age-dependent exponential transition rate $\nu(t)$ for conversion from normal tissue to BE as

$$\nu(t) = \nu_0 [(1 - p_G(t)) - RR \cdot p_G(t)]$$

where RR is the relative risk for GERD given BE.

The density for BE onset times, $f_{BE}(t)$ and cumulative function for BE prevalence $F_{BE}(t)$ are

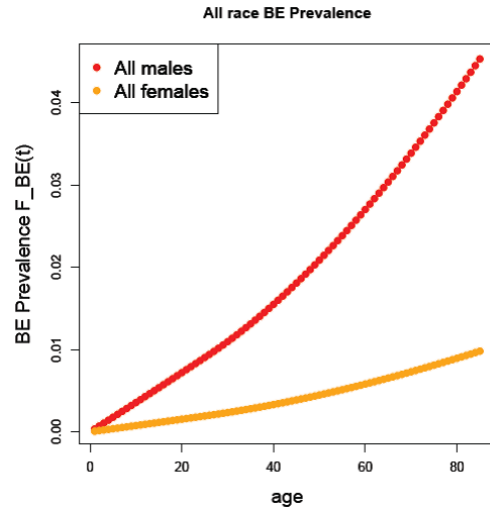
$$f_{BE}(t) = \nu(t) e^{-\int_0^t \nu(u) du},$$

and

$$F_{BE}(t) = 1 - e^{-\int_0^t \nu(u) du}, \text{ respectively.}$$

As described in the Background section, different studies differ in their estimates of

relative risk (RR) for BE given GERD.^{8,9,10} We use a consensus estimate of RR from these studies in assuming a model relative risk of RR=5 for BE given GERD.

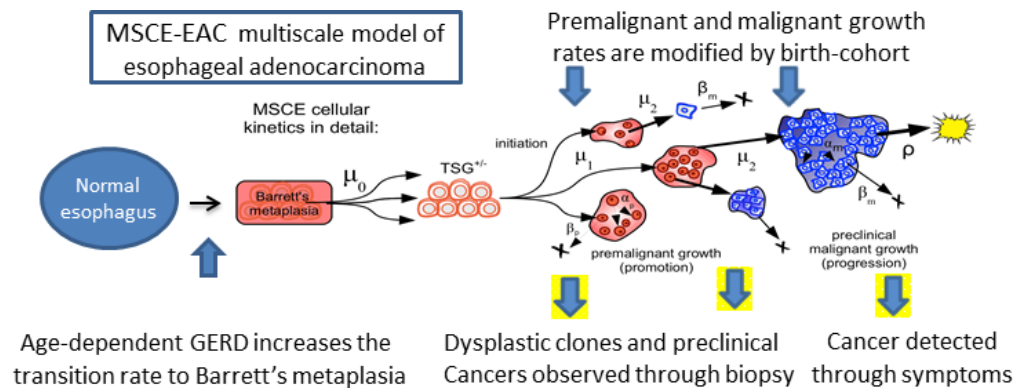


Model BE prevalence based on RR=5

We note that the primary MSCE–EAC model outcome is EAC and the model assumes BE is necessary for EAC. Using the estimate of RR=5, we used maximum likelihood methods to calibrate the MSCE–EAC model to EAC incidence data from SEER to estimate the remaining model parameters.

BE is modeled as a metaplastic tissue with random segment length drawn from a beta distribution $B(16/11, 4)$ ¹³ containing on average 106 BE stem cells. These BE stem cells may undergo mutation or epigenetic modification, with two successive hits occurring during asymmetric cell division (at rates μ_0, μ_1) that are required to inactivate a gatekeeper or tumor suppressor gene (TSG) and generate a premalignant daughter cell with partial loss of tissue homeostasis. (When calibrating to EAC incidence, μ_0 and μ_1 are not separately identifiable, so without loss of generality we set $\mu_0 = \mu_1$). Premalignant cells, which we associate with high grade dysplasia (HGD) may divide (with rate α_p); die, undergo apoptosis or differentiate (at rate β_p); or mutate during asymmetric cell division (at rate μ_2) to generate a malignant cell. Similarly, malignant cells may divide (with rate α_m); undergo apoptosis or differentiate (at rate β_m); or undergo detection through a size–based stochastic observation process based on a per–cell detection rate ρ .

The difference between the birth and death rates is called the net cell proliferation rate (γ) for each cell type. Model parameters are calibrated through maximum likelihood fits to EAC incidence data from nine registries of the Surveillance and End Results (SEER) database between 1975 and 2010.¹



EAC incidence has increased approximately six-fold in the US since 1975.^{1,12} These temporal trends were modeled by systematically applying flexible period and cohort trends to the biological parameters of the MSCE-EAC model, and using likelihood methods for model comparison and selection of the best model fit to SEER incidence. The best fitting model includes a sigmoidal birth cohort effect modifying the growth rates of premalignant and malignant cells, with rates for malignant growth significantly larger than for premalignant growth. The sigmoidal shape for premalignant growth rate is parametrized as shown in the following section.

Growth of premalignant (P–cells) modified by sigmoidal birth–cohort effect

Let b_k represent the birth cohort, indexed by year k .

NOTE: to keep notation simple in the following, we do not add the index k to the division rates α_P or α_M , net cell proliferation rates γ_P or γ_M , or death rates β_P or β_M (where P and M represent premalignant and malignant cells, respectively).

$$\alpha_P = \alpha_{P0} \left(g_1 + \frac{2}{1 + \exp(-g_2(b_k - t_{ref}))} \right) \quad \text{'P cell division'}$$

$$\gamma_P = \gamma_{P0} \left(g_1 + \frac{2}{1 + \exp(-g_2(b_k - t_{ref}))} \right) \quad \text{'Net P-cell proliferation rate'}$$

$$\beta_P = \alpha_P - \gamma_P - \mu_2 \quad \text{'P-cell death (apoptosis) or differentiation rate'}$$

Growth of malignant M–cells modified by sigmoidal birth–cohort effect

$$\alpha_M = \alpha_{M0} \left(g_1 + \frac{2}{1 + \exp(-g_2(b_k - t_{ref}))} \right) \quad \text{'M-cell division rate'}$$

$$\gamma_M = \gamma_{M0} \left(g_1 + \frac{2}{1 + \exp(-g_2(b_k - t_{ref}))} \right) \quad \text{'Net M-cell proliferation rate'}$$

$$\beta_M = \alpha_M - \gamma_M - \rho \quad \text{'M-cell death (apoptosis) or differentiation rate'}$$

The analytic form of the sigmoidal function allows smooth estimation of future trends, with projections until 2030 for males and females shown in the figures below. The figures show that the six-fold increase in incidence can be explained by smaller changes in the net cell proliferation rates of premalignant and malignant clones that increase less than three-fold across birth cohorts spanning a century.

MSCE-EAC Model Differential Equations

$$\frac{dy_1}{dt} = \beta_M - (\alpha_M + \beta_M + \rho) y_1 + \alpha_M y_1^2$$

$$\frac{dy_2}{dt} = 2 \alpha_M y_1 y_2 - (\alpha_M + \beta_M + \rho) y_2$$

$$\frac{dy_3}{dt} = \beta_P + \mu_2 y_1 y_3 - (\alpha_P + \beta_P + \mu_2) y_3 + \alpha_P y_3^2$$

$$\frac{dy_4}{dt} = 2 \alpha_P y_3 y_4 + \mu_2 (y_4 y_1 + y_3 y_2) - (\alpha_P + \beta_P + \mu_2) y_4$$

$$\frac{dy_5}{dt} = \mu_1 y_5 (y_3 - 1)$$

$$\frac{dy_6}{dt} = \mu_1 (y_6 y_3 - y_6 + y_5 y_4)$$

$$\frac{dy_7}{dt} = X \mu_0 y_7 (y_5 - 1)$$



$$\frac{dy_8}{dt} = X \mu_0 (y_8 y_5 - y_8 + y_7 y_6)$$

$$\frac{dy_9}{dt} = \nu y_9 (y_7 - 1) \quad \text{'Survival = } S(t) = y_9 \text{'}$$

$$\frac{dy_{10}}{dt} = -\nu y_8 \quad \text{'Hazard = } h(t) = y_{10} \text{'}$$

MSCE-EAC Model Likelihood

Maximum likelihood methods were used to fit to EAC incidence data from SEER for ages 1 to 84 and calendar years 1975–2010.

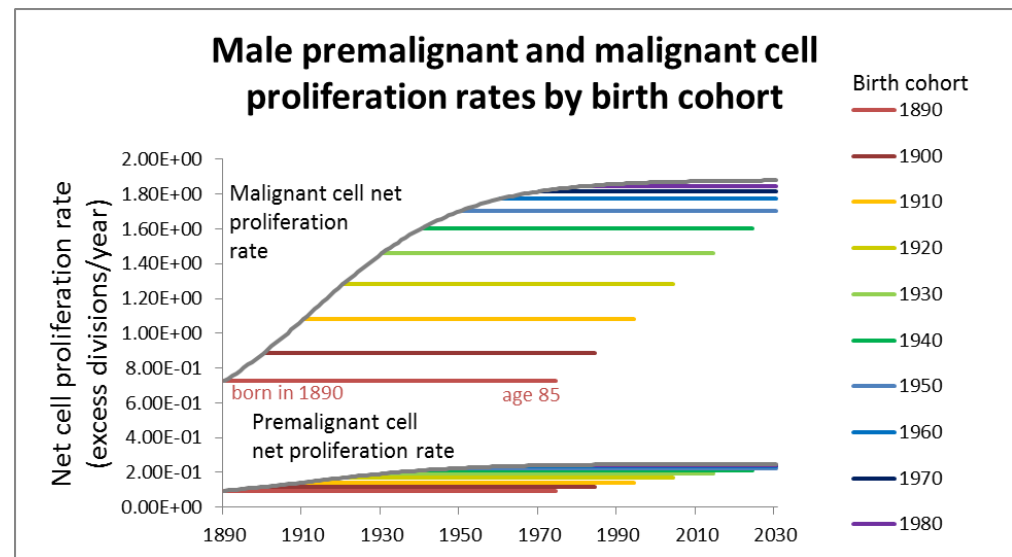
The expected number of EAC cancers at age a_i and period (calendar year) p_j and birth cohort $b_k = c_j - a_i$ is

$\Lambda_{i,j} = PY_{i,j} h(a_i, b_k)$, where $PY_{i,j}$ is the number of person years of age a_i and period p_j , and the birth-cohort specific hazard is $h(a_i, b_k) = h(t)|\{t = a_i, b_k\}$.

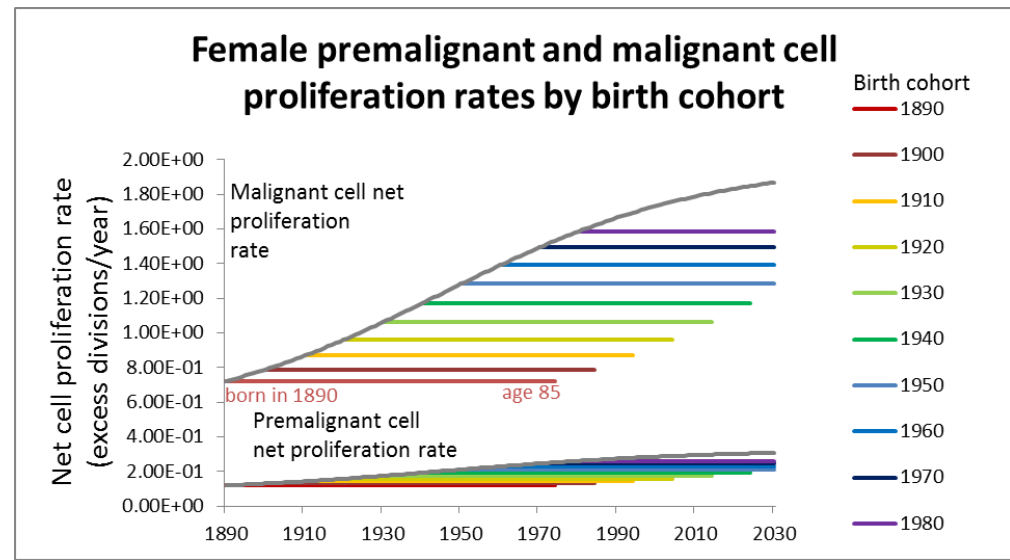
The likelihood is

$$\mathcal{L} = \prod_{i,j} \frac{\Lambda_{i,j}^{O_{i,j}} \exp[-\Lambda_{i,j}]}{O_{i,j}!}, \text{ where } O_{i,j} \text{ is the number of observed EAC cases for age } a_i \text{ and period } p_j.$$

The best model fit includes a sigmoidal (birth) cohort trend on both premalignant and malignant clonal expansion, with rates for malignant growth significantly larger than for premalignant growth.



Of particular note is the observation that the estimated increases in proliferation rates among males are leveling off for recent birth cohorts but continue rising for recent females birth cohorts.



CONTRIBUTORS

Bill Hazelton, Kit Curtius, Georg Luebeck

REFERENCES:

- 1 SEER "Surveillance, Epidemiology, and End Results (SEER) Program (www.seer.cancer.gov) SEER*Stat Database: Incidence – SEER 9 Regs Research Data, Nov 2011 Sub (1973–2010) 2010; "
- 2 Ruigomez, A., Wallander, M. A., Lundborg, P., Johansson, S., Rodriguez, L. A. G. "Gastroesophageal reflux disease in children and adolescents in primary care." in *Scand J Gastroenterol* 2010; 45: 2: 139–146
- 3 Ruigomez, A., Rodriguez, L. A. G., Wallander, M. A., Johansson, S., Graffner, H., Dent, J. "Natural history of gastro-oesophageal reflux disease diagnosed in general practice" in *Alimentary Pharmacology & Therapeutics* 2004; 20: 7: .751–60.
- 4 Talley, N. J., Zinsmeister, A. R., Schleck, C. D., Melton, L. J., 3rd "Dyspepsia and Dyspepsia Subgroups – a Population-Based Study" in *Gastroenterology* 102: 4 Pt 1: 1259–68
- 5 Locke, G. R., 3rd, Talley, N. J., Fett, S. L., Zinsmeister, A. R., Melton, L. J., 3rd "Prevalence and clinical spectrum of gastroesophageal reflux: a population-based study in Olmsted County, Minnesota." in *Gastroenterology* 1997; 112: 5: 1448–56
- 6 Locke, G. R., 3rd, Talley, N. J., Fett, S. L., Zinsmeister, A. R., Melton, L. J., 3rd "Risk factors associated with symptoms of gastroesophageal reflux" in *Am J Med* 1999; 106: 6: 642–9
- 7 Dent, J., El-Serag, H. B., Wallander, M. A., Johansson, S "Epidemiology of gastro-oesophageal reflux disease: a systematic review." 2005; 54: 5: 710–7
- 8 Thrift, A. P., Kramer, J. R., Qureshi, Z., Richardson, P. A., El-Serag, H. B. "Age at onset of GERD symptoms predicts risk of Barrett's esophagus." in *American Journal of Gastroenterology* 2013; 108: 6: 915–922
- 9 Taylor, J. B., Rubenstein, J. H. "Meta-analyses of the effect of symptoms of gastroesophageal reflux on the risk of Barrett's esophagus" in *Am J Gastroenterol* 2010; 105: 8: 1729–37
- 10 Rubenstein, J. H., Taylor, J. B. "Meta-analysis: the association of oesophageal adenocarcinoma with symptoms of gastro-oesophageal reflux" in *Aliment Pharmacol Ther* 2010; 32: 10: 1222–7



- 11 Falk, G. W., Jacobson, B. C., Riddell, R. H., Rubenstein, J. H., El-Zimaity, H., Drewes, A. M., Roark, K. S., Sontag, S. J., Schnell, T. G., Leya, J., Chejfec, G., Richter, J. E., Jenkins, G., Goldman, A., Dvorak, K., Nardone, G. "Barrett's esophagus: prevalence–incidence and etiology–origins." in *Ann N Y Acad Sci* 2011; 1232: : 1–17
- 12 Kong, C. Y., Kroep, S., Curtius, K., Hazelton, W. D., Jeon, J., Meza, R., Heberle, C. R., Miller, M. C., Choi, S. E., Lansdorp–Vogelaar, I., van Ballegooijen, M., Feuer, E. J., Inadomi, J. M., Hur, C., Luebeck, E. G. "Exploring the Recent Trend in Esophageal Adenocarcinoma Incidence and Mortality Using Comparative Simulation Modeling." in *Cancer Epidemiol Biomarkers Prev* 2014; 23: 6: 997–1006
- 13 Wikipedia "Beta distribution" in http://en.wikipedia.org/wiki/Beta_distribution 2014;



ASSUMPTION OVERVIEW

SUMMARY

We assume that EAC develops from BE through GERD and non-GERD pathways, with subsequent steps described by a multistage cell-based model. The primary calibration of cell kinetic parameters in the MSCE-EAC model is done through maximum likelihood fits to SEER data. Only specific combinations of cell kinetic parameters are identifiable from incidence data.

BACKGROUND

The model represents the transition from normal esophageal squamous tissue to metaplastic BE tissue as a Poisson process with a rate that is higher for individuals with GERD compared to individuals without GERD.

Following generation of a BE segment in some individuals, a multistage carcinogenesis process is used to represent stochastic cellular processes of sequential mutation, clonal expansion to generate hyperplastic tissue, further mutation to malignant status, clonal growth of the malignant tissue, and detailed observation processes, including biopsy sampling, and treatment, including radio-frequency ablation (RFA).

ASSUMPTION LISTING

1. The transition from normal squamous epithelium to BE tissue is a field effect with a transition rate that depends on GERD status.

The normal to BE transition is modeled as a Poisson process with changing rates that depends on GERD onset age. This approach is used to represent a 'field' effect transition, in which a region (or field) of tissue makes the transition during a short interval of time. This assumption appears consistent with available observational data that suggests that BE tissue segments do not generally change significantly in size subsequent to their first detection.

2. We use a three stage model with two rate-limiting mutations that occur prior to premalignant clonal expansion, and a subsequent mutation that generates the malignant phenotype.

The assumption of two initial mutations is consistent with the tumor suppressor paradigm that requires two genetic or epigenetic changes to enter the premalignant phase of carcinogenesis. This is in contrast to the two-stage clonal expansion (TSCE) model that assumes a single mutation prior to clonal expansion. (The TSCE model has a different asymptotic behavior for the hazard at very old ages that tends to plateau). Earlier testing of TSCE versus three-stage models indicated that the three-stage models provide better fits to the digestive-tract (esophageal, stomach, pancreatic, and colorectal) cancers. Although models with more initial mutations are possible, a mathematical analysis indicates that models with two or more mutations prior to clonal expansion have nearly indistinguishable shapes when the product of the initial mutations remain the same. However, if a larger number of initial mutations is assumed, then the mutation rates are forced to become more rapid, and at some point this becomes biologically implausible. These results provide the basis for use of the three stage model.

3. We assume that cells in BE tissue progress independently along the pathway to cancer through birth, death, and mutation processes



Cells on the pathway to cancer are assumed to arise in the BE tissue and progress independently through a stochastic birth, death, mutation, and observation processes for both premalignant and malignant cells, as specified by a multistage model.

4. We assume each premalignant clone begins as low grade dysplasia (LGD), but as the clone grows it may undergo a stochastic transition to become a high grade dysplasia (HGD) clone.

Any of the premalignant cells in LGD or in HGD may undergo malignant transformation, starting the growth of an Esophageal adenocarcinoma (EAC) clone. The model simulates a transition from LGD to HGD using a transition rate that increases in proportion to the number of premalignant cells in the clone. Thus an individual with BE may have multiple clones of different size, some classified as LGD and others as HGD, and EAC clone(s) may begin within any of the LGD or HGD clones.

5. We assume that the number of stem cells in BE has a fixed value per unit area of BE tissue, and that the first two mutations following BE onset occur at equal rates.

Only certain cell kinetic parameter combinations in the multistage model are identifiable through fits to incidence. Identifiable combinations include the net cell proliferation rate for premalignant cells, the product of the number of stem cells and the first two mutation rates, and the product of the premalignant cell division rate and the mutation rate of these cells to become malignant. Thus some assumptions are required to specify non-identifiable parameters. In particular, we assume equality of the first two mutation rates, and set the number of stem cells to values consistent with the available literature. Cell division rates are only weakly identifiable, and were initially set to biologically plausible values. These assumptions were tested through secondary calibration using detailed spatial simulation methods to fit observations from clinical biopsy outcomes, including number and size of LGD, HGD, and pre-clinical EAC clones.

6. The cancer detection process in the multistage model is represented using a stochastic observation process that assumes each cell contributes independently to the detection probability, collectively leading to a size based detection probability.

This size-based observation process generally seems reasonable, as the detection parameter ρ can be adjusted to reflect the median size of tumor at detection. However, the distributional properties of tumor size at detection may not be identical to that seen in clinical practice.

7. Clones generated through the multistage process are assumed to occur at random within the BE segment.

This assumption is necessary because multistage process itself does not include information on the spatial location of clones, only the number and sizes of clones. Simulated clones generated through the multistage process are placed at random on a 2-D surface sized to reflect the BE segment within the esophagus.

8. We assume that LGD, HGD, or EAC detection occurs when biopsied tissue contains cell counts for LGD, HGD, or EAC that exceed specific threshold values.

The predicted biopsy detection process for LGD, HGD or EAC depends on the physical size of clones and the assumed fraction of biopsy tissue required to make a positive identification of HGD or EAC. Several parameters, including fraction of biopsy tissue required for detection, the number of stem cells per unit area, and the division rate of premalignant cells (a weakly identifiable parameter) were evaluated and compared with clinical reports on the detection frequencies for finding HGD and EAC in BE



patients.

9. We assume a per-cell detection probability for symptomatic EAC diagnosis of

$$\rho = 1.0e^{-9}.$$

This specifies that the median size of an EAC at symptomatic detection will contain approximately 10^9 cancer cells.

PARAMETER OVERVIEW

SUMMARY

Most of the model parameters were estimated through maximum likelihood fits to EAC incidence data from nine registries of the Surveillance, Epidemiology, and End Results (SEER) database by single year of age (20 – 84) and calendar year (1975 – 2010). However, some parameters must be fixed initially to achieve parameter identifiability.

BACKGROUND

Key biological parameter combinations may be deduced from the shape of the cancer incidence curve, described mathematically by a hazard function. The incidence curve may be broken into sections representing an exponential–then–linear character of the multistage hazard function as a function of age at diagnosis.

PARAMETER LISTING OVERVIEW

The slope of the linear phase is $\lambda \equiv \mu_0 X \mu_1 p_\infty$ and the growth parameter of the exponential phase $g_p \equiv \alpha_p - \beta_p - \mu_2$. However, the rates μ_0 and μ_1 cannot be estimated separately because the slope λ depends on their product. Analogous to premalignant growth, the malignant growth parameter $g_M \equiv \alpha_M - \beta_M - \rho$. To identify the malignant conversion rate and detection rate per cell, μ_2 and ρ respectively, it is necessary to fix the cell division rates α_p and α_M . Although the product $\alpha_M \rho$ is mathematically identifiable, we were not able to obtain stable estimates and therefore also fixed the (per cell) cancer detection parameter $\rho = 10^{-9}$, which corresponds to median symptomatic detection of EACs when they contain approximately $n \sim 10^9$ cancer cells (see [Assumption Overview](#)).

We compared multiple models by fixing $g_{M,0}$ and detection rate ρ to different values in order to achieve reasonable mean sojourn times and tumor doubling times that are in line with clinical data. In these Results, the EAC clinical detection rate $\rho = 10^{-9}$ per cell/year, malignant cell proliferation rate $g_{M,0} = 0.75$ per cell/year, and $X = 10^6$ stem cells in an average 5 cm BE segment.

Maximum likelihood methods were used to estimate values for $g_{P,0}, g_1, g_2, g_3$ (reference year), where t_b = birth cohort year, that best explain the temporal trends for EAC incidence in terms of sigmoidal birth cohort trends affecting promotion:

$$g_p = g_{P,0} \left(g_1 + \frac{2}{1 + e^{(-g_2(t_b - g_3))}} \right), \quad g_M = g_{M,0} \left(g_1 + \frac{2}{1 + e^{(-g_2(t_b - g_3))}} \right)$$

$$\alpha_p = \alpha_{P,0} \left(g_1 + \frac{2}{1 + e^{(-g_2(t_b - g_3))}} \right), \quad \alpha_M = \alpha_{M,0} \left(g_1 + \frac{2}{1 + e^{(-g_2(t_b - g_3))}} \right)$$

$$g_p = \alpha_p - \beta_p - \mu_2, \quad g_M = \alpha_M - \beta_M - \rho$$

Value (95% CI)	Males	Females
ν_0	3.65 (3.19 – 4.13) $\times 10^{-4}$	7.48 (4.87 – 10.29) $\times 10^{-5}$
$\mu_0(\mu_1)$	7.99 (6.38 – 9.83) $\times 10^{-4}$	7.05 (6.13 – 12.25) $\times 10^{-4}$
μ_2	4.54 (3.65 – 6.47) $\times 10^{-5}$	6.89 (3.16 – 14.28) $\times 10^{-5}$
$g_{P,0}$	9.91 (9.28 – 10.99) $\times 10^{-2}$	1.23 (1.06 – 1.35) $\times 10^{-1}$
g_1	5.09 (2.75 – 5.90) $\times 10^{-1}$	6.40 (2.16 – 8.44) $\times 10^{-1}$
g_2	5.38 (4.83 – 5.72) $\times 10^{-2}$	2.98 (2.47 – 3.44) $\times 10^{-2}$
g_3	1912.5 (1909.1 - 1914.1)	1945.3 (1923.9 - 1954.4)

Table S1: MSCE-EAC model parameters All parameter estimates have the units of per cell per year. Markov Chain Monte-Carlo 95% confidence intervals provided beside the maximum likelihood estimates.



COMPONENT OVERVIEW

SUMMARY

The MSCE–EAC model includes six components, consisting of a model of symptomatic gastroesophageal disease (sGERD), an analytic multistage clonal expansion model hazard for BE and EAC incidence, a temporal trends component, a hybrid stochastic simulation component, a biopsy screening module, and a radio–frequency ablation (RFA) treatment module.

OVERVIEW

The sGERD component was calibrated to sGERD incidence data and age–adjusted sGERD prevalence data from the US and UK to generate estimates of age–dependent sGERD prevalence by gender. The sGERD prevalence influences the rate of transition to BE, and more importantly, the premalignant clonal expansion rate (net growth rate for high grade dysplasia, or HGD) in the multistage model. The multistage model (MSCE–EAC) hazard was calibrated to EAC incidence in SEER, and describes the biological process of transition to BE in the esophagus, and the multistage carcinogenesis process culminating in EAC. The temporal trends component was used to estimate the maximum likelihood period and birth–cohort trends affecting biological processes, including onset of BE and premalignant promotion, for dates ranging from 1890–2010. The hybrid stochastic simulation component was used to provide realizations of HGD and malignant clones in individuals as they age. The biopsy screening module represents biopsy of HGD and malignant clones through quadrant sampling using forceps, which is referred to as the Seattle Protocol. RFA treatment, which is used in patients diagnosed with BE and HGD, is modeled using a module that allows specific proportions of cells of different types to be eliminated during RFA treatment, and then to assess the results on expected diagnoses of HGD and EAC during subsequent years.

COMPONENT LISTING

sGERD component

We modeled gastroesophageal reflux disease (GERD) symptom prevalence at age t , $p_{sGERD}(t)$, based on data from Ruigomez, et al. for incidence (by 2–year age intervals) of GERD symptoms (that occur weekly or more frequently) among children (n=1700), ¹ and another study by Ruigomez, et al. ² on incidence of weekly GERD symptoms among adults (n=1996) with data provided in 10 year intervals.

We used maximum likelihood methods to fit parameters for a GERD prevalence model separately for males and females, using a transition rate to GERD prevalence based on the GERD incidence data and estimating a back–transition rate (representing recovery from GERD) to fit an assumed 20% target rate for age–adjusted GERD prevalence between ages 40–85. See [GERD Model Component](#) for further detail.

Analytic multistage clonal expansion (MSCE) model hazard component

Analytically construct the hazard function of the MSCE–EAC model which consists of two stochastic processes: the random occurrence of BE and the multistage carcinogenesis process arising in BE. Parameters were estimated using maximum likelihood methods. Mathematically, the MSCE–EAC branching process' probability density function (pdf) may be written as a convolution of the BE conversion density f_{BE} (assumed to be exponential) and the MSCE model density after BE onset (f_{BE-MS}) as



$f_{MSCE}(t) = \int_0^\infty f_{BE}(u)f_{BE-MS}(t-u)u$. Further details are provided in the [Model Overview](#) section.

Temporal trends component

This component was used to estimate the mechanistic role of symptomatic GERD (sGERD) and other factors (OF) in driving the observed U.S. trends, and was accomplished in two phases. Phase 1 focused on identifying important biological mechanisms that are likely driving the observed EAC trends. Phase 2 focused on understanding the mechanistic role of sGERD and OF in acting through the biological processes identified in Phase 1 to drive EAC incidence. Both phases of model development were informed by EAC incidence data from SEER, sGERD incidence data from the UK, and US sGERD prevalence data. Separate multiscale models of EAC incidence were built for all-race men and women. See [Temporal Trends Component](#) for further detail.

Hybrid stochastic simulation component

The simulation begins with generation of individual BE onset times, BE segment lengths for each patient (which determines the number of BE stem cells), and generation of pre-initiated and initiated stem cells using Poisson rate-limiting mutation with rate μ_0 and μ_1 , respectively. Initiated premalignant clones undergo independent birth-death-mutation (b-d-m) processes that we simulate to track cell count and times of malignant transformations. See [Stochastic Simulation Component](#) for further detail.

Biopsy screening module

For simulations following the Seattle biopsy protocol, the BE segment can be visualized as partitioned into identical rectangular sections, which we will call "biopsy quadrants" with a single biopsy in the center of the quadrant. For example, an average BE segment of length 5 cm and 7.5 cm circumference will have 12 biopsy quadrants, 3 levels of length 5/3 cm with 4 quadrant biopsies each. Furthermore, we assume periodic boundary conditions when placing clones in a random quadrant.

To account for different biopsy protocols, incompletely described histological methods, and inter-observer variation of neoplasia grade, we present results from the computational model for different levels of diagnostic sensitivity based on the minimum number of neoplastic (pre-malignant/malignant) crypts within a simulated biopsy specimen required for pathologic diagnosis of dysplasia/malignancy among BE patients without prior diagnosis of EAC.

After a simulated screen of BE patients for detection of LGD, HGD, and preclinical EAC at age t_s , the MSCE-EAC model can be used to further simulate an intervention such as an ablative treatment using radio frequency.

Radio-frequency ablation component

After a simulated screen of BE patients for detection of dysplasia and preclinical EAC at age t_s , the MSCE-EAC model can be used to further simulate an intervention such as an ablative treatment using radio frequency. To replicate current practice with radio frequency ablation (RFA), we first remove the prevalent EAC cases that were screen detected at the index endoscopy and then simulate RFA treatment on positively screened patients with dysplasia. The MSCE-EAC model can then be used to project



the EAC incidence and age-specific prevalence of dysplasia into the future after an ablative treatment. The ablation is assumed to curatively reduce all clonal populations and the number of BE crypts by certain percentages as described in the following. As a simple example, we consider the model's predictions after a single ablative treatment when indicated by the presence of high grade dysplasia on future EAC incidence.

REFERENCES:

- ¹ Ruigomez, A., Wallander, M. A., Lundborg, P., Johansson, S., Rodriguez, L. A. G. "Gastroesophageal reflux disease in children and adolescents in primary care." in *Scand J Gastroenterol* 2010; 45: 2: 139-146
- ² Ruigomez, A., Rodriguez, L. A. G., Wallander, M. A., Johansson, S., Graffner, H., Dent, J. "Natural history of gastro-oesophageal reflux disease diagnosed in general practice" in *Alimentary Pharmacology & Therapeutics* 2004; 20: 7: .751-60.



OUTPUT OVERVIEW

SUMMARY

The model outputs range from estimated trends for incidence and mortality, mechanistic factors driving these trends, simulations of biopsy based screening, and treatment through radio-frequency ablation.

OVERVIEW

Outputs from the model include projections of incidence and mortality for US males and females by birth cohort and calendar year, trends for symptomatic gastroesophageal reflux disease (sGERD) in the US, biological parameters of the multistage process that are driving EAC incidence, mechanistic influences of sGERD and other factors (OF) over time, and detailed stochastic simulations of the multistage clonal expansion process.

OUTPUT LISTING

Incidence and mortality trends

US male and female incidence and mortality trends for all-races and whites for males and females – calibrated to SEER data between 1975 and 2010, and ages 20–84

sGERD trends

Trends for symptomatic gastroesophageal reflux disease (sGERD) in the US – consistent with cross-sectional sGERD incidence and prevalence with longer term trends estimated by fitting to SEER EAC incidence

Biological parameters of the multistage process that are driving EAC incidence

Estimated through maximum likelihood fits to SEER data

Mechanistic influences of sGERD and other factors (OF) over time

Fit through extensive maximum likelihood estimation (MLE) and Markov chain Monte Carlo (MCMC) methods to fit SEER incidence data

Joint distribution of premalignant and malignant clones

Detailed stochastic simulations of the multistage clonal expansion process provide explicit realizations of the joint distribution of premalignant and malignant clones using parameters derived through maximum likelihood fitting to SEER incidence data

Costs and life years gained

A simulator of biopsy screening among males and females under different biopsy screening protocols provides estimates of costs and life years gained through different screening protocols.

Reduction or delay of LGD, HGD, and EAC

The simulator estimates the impact of radio-frequency ablation on reducing or delaying the occurrence of LGD, HGD and EAC.



RESULTS OVERVIEW

SUMMARY

Results from the model include estimates for rates and trends for biological processes occurring during EAC carcinogenesis, sensitivities of biopsy protocols, and the impact of radio-frequency ablation (RFA), including the effects of 'touch-up' treatments when the initial treatment was not fully successful.

OVERVIEW

Results from the model include a study on how trends for symptomatic gastroesophageal reflux disease (sGERD) and other factors (OF) in the US may influence biological parameters of the multistage process to drive EAC incidence trends.¹ Similarly, the methods describing the detailed stochastic simulations of the multistage clonal expansion process, and illustration of explicit realizations of the joint distribution of premalignant and malignant clones and simulation of biopsy screening and sensitivity for detection of HGD and EAC are currently under review in a separate manuscript.

RESULTS LIST

Calibration of EAC incidence and incidence-based mortality to SEER data and projection of trends to year 2030

Maximum likelihood methods were used to calibrate the FHCRC model to GERD incidence data and SEER data. These methods provided excellent fits to the SEER data for US incidence and incidence-based mortality for calendar years 1975–2010 and by single-year birth cohorts. During model development, the FHCRC modeling group compared different models using maximum likelihood methods, finding that the premalignant clonal expansion rate differs significantly by birth cohort. The best fit to the data was found using a sigmoidal birth cohort function influencing the premalignant clonal expansion rate.^{2,3}

The calibrated FHCRC model results indicate that there were 81,069 expected male EAC deaths and 10,375 expected female deaths between 1991–2020. Incidence and mortality trends were projected to year 2030 by utilizing birth-cohort specific parameters, with separate projections for local, regional, and distant staged tumors. These projections suggest that male incidence trends are continuing upward, but show a marked flattening trend, reflecting a decreasing birth-cohort trend for later birth cohorts. Trends for females also continue upward to 2030, but unlike for males, there is no significant flattening of the projected trends. Projections of the FHCRC model to 2030 predict that there will be approximately 81,069 male EAC deaths and 10,375 female deaths between 2011–2030.²

The EAC sojourn time may differ by birth cohort

For the FHCRC model, the EAC sojourn time represents the time between appearance of the first malignant cell that doesn't become extinct and the incidental detection of EAC. (This differs from other CISNET models that estimate the time from smallest clinically detectable lesion to EAC incidence). The birth cohort influence on the clonal expansion rates directly influences the expected clonal extinction probability and the expected EAC sojourn time. The FHCRC model predictions for EAC sojourn time range from ~18 years for the 1900 birth cohort, to < 10 years for recent birth cohorts.

Impact of symptomatic GERD and other factors on explaining EAC trends

Biologically based modeling of the mechanistic impact of symptomatic GERD and other factors in fitting to EAC incidence data and GERD incidence data suggests that at most, ~16% of the observed 6-fold increase in EAC incidence between 1975 and 2009 is attributable to GERD, with the remainder explained by other factors. The modeling suggests that GERD influences the transition to BE, but more importantly, GERD increases the rate of premalignant promotion. The other factors also appear to primarily influence premalignant promotion.¹

Dependence of HGD detection and the probability of missed malignancy on the biopsy sampling sensitivity

Detailed simulation of biopsy sampling according to the Seattle protocol suggests that the probability of detecting HGD depends strongly on the percent of biopsy tissue used for analysis, with sensitivities for HGD ranging from ~2–9% for males with sampling percentages ranging from 10–95%. For females, the probability of HGD detection is lower, ranging from ~1–6% for biopsy sampling percentages ranging from 10–95%. The probability of missed malignancy during biopsy sampling ranges from ~20% with 10% biopsy sampling among males, and ~15% among females; to ~5% for males and ~4% for females at 95% sensitivity.³

The predicted impact of ablation in reducing EAC depends on the cell types ablated and the ablation efficiency

Detailed simulations of the lifetime impact of ablation on cumulative EAC incidence was done assuming different scenarios for the efficacy of ablation, with sensitivity analyses comparing elimination of 50%, 99%, and 100% of all cell types, only HGD cells, or only malignant cells. The results indicate that ablation of 100% of HGD and malignant cells delays the expected incidence curve by approximately seven years, with smaller effects seen for less efficient ablation or ablation of selected cell types.^{4,5}

REFERENCES:

- 1 Hazelton William D., Curtius Kit, Inadomi John M., Vaughan Thomas L., Meza Rafael, Rubenstein Joel H., Hur Chin and Luebeck E. Georg. "The Role of Gastroesophageal Reflux and Other Factors during Progression to Esophageal Adenocarcinoma" in *Cancer Epidemiology, Biomarkers and Prevention* 2015; 24: : 1012-1023
- 2 Kong, C. Y., Kroep, S., Curtius, K., Hazelton, W. D., Jeon, J., Meza, R., Heberle, C. R., Miller, M. C., Choi, S. E., Lansdorp-Vogelaar, I., van Ballegooijen, M., Feuer, E. J., Inadomi, J. M., Hur, C., Luebeck, E. G. "Exploring the Recent Trend in Esophageal Adenocarcinoma Incidence and Mortality Using Comparative Simulation Modeling." in *Cancer Epidemiol Biomarkers Prev* 2014; 23: 6: 997-1006
- 3 Curtius, Kit, Hazelton WD, Jeon J, Luebeck EG "A multiscale model evaluates screening for neoplasia in Barrett's Esophagus." in *PLOS Computational Biology* 2015; 11: 5: e1004272
- 4 Heberle CR, Omidvari AH, Ali A, Kroep S, Kong CY, Inadomi JM, Rubenstein JH, Tramontano AC, Dowling EC, Hazelton WD, Luebeck EG, Lansdorp-Vogelaar I, Hur C "Cost-Effectiveness of Screening Patients with Gastroesophageal Reflux Disease for Barrett's Esophagus With a Minimally Invasive Cell Sampling Device" in *Gastroenterol Hepatol* 2017; S1542-3565: 17: 30197-0
- 5 Kroep S, Heberle CR, Curtius K, Kong CY, Lansdorp-Vogelaar I, Ali A, Wolf WA, Shaheen NJ, Spechler SJ, Rubenstein JH, Nishioka NS, Meltzer SJ, Hazelton WD, van Ballegooijen M, Tramontano AC, Gazelle GS, Luebeck EG, Inadomi JM, Hur C "Impact of Radiofrequency Ablation Treatment of Barrett's Esophagus on Esophageal Adenocarcinoma: A Comparative Modeling Analysis." in *Clin Gastroenterol Hepatol* 2017; 1542-3565: 17: 30019-8



GERD MODEL COMPONENT

SUMMARY

Gastroesophageal Reflux Disease (GERD) Model

OVERVIEW

sGERD component

We modeled gastroesophageal reflux disease (GERD) symptom prevalence at age t , $p_{sGERD}(t)$, based on data from Ruigomez, et al. for incidence (by 2-year age intervals) of GERD symptoms (that occur weekly or more frequently) among children (n=1700),¹ and another study by Ruigomez, et al.² on incidence of weekly GERD symptoms among adults (n=1996) with data provided in 10 year intervals.

DETAIL

We used maximum likelihood methods to fit parameters for a GERD prevalence model separately for males and females, using a transition rate to GERD prevalence based on the GERD incidence data and estimating a back-transition rate (representing recovery from GERD) to fit an assumed 20% target rate for age-adjusted GERD prevalence between ages 40–85. We then found that we could achieve excellent fits to these data by simplified (3 parameter) gender-specific models representing a (slower) transition rate among children, a transition age, and an adult rate for acquiring weekly GERD symptoms (See [Model Overview](#)).

BE prevalence $F_{BE}(t)$ can be estimated, via parameter ν_0 by fitting to SEER data and fixing a value for relative risk $RR \in \{5, 10, 15\}$, given the model for GERD prevalence as described in the main text with the BE conversion rate,

$$\nu(t) = \nu_0 \left((1 - p_{sGERD}(t)) + RR \cdot p_{sGERD}(t) \right)$$

$$\Rightarrow F_{BE}(t) = \Pr[T_{BE} \leq t] = 1 - e^{-\int_0^t \nu(s) ds}$$

REFERENCES:

- ¹ Ruigomez, A., Wallander, M. A., Lundborg, P., Johansson, S., Rodriguez, L. A. G. "Gastroesophageal reflux disease in children and adolescents in primary care." in *Scand J Gastroenterol* 2010; 45: 2: 139-146
- ² Ruigomez, A., Rodriguez, L. A. G., Wallander, M. A., Johansson, S., Graffner, H., Dent, J. "Natural history of gastro-oesophageal reflux disease diagnosed in general practice" in *Alimentary Pharmacology & Therapeutics* 2004; 20: 7: 751-60.



TEMPORAL TRENDS COMPONENT

SUMMARY

Esophageal Adenocarcinoma incidence has increased over six-fold in the U.S. since 1975.

OVERVIEW

This component was used to estimate the mechanistic role of symptomatic GERD (sGERD) and other factors (OF) in driving the observed U.S. trends, and was accomplished in two phases.

Phase 1 focused on identifying important biological mechanisms that are likely driving the observed EAC trends.

Phase 2 focused on understanding the mechanistic role of sGERD and OF in acting through the biological processes identified in Phase 1 to drive EAC incidence. Both phases of model development were informed by EAC incidence data from SEER, sGERD incidence data from the UK, and US sGERD prevalence data. Separate multiscale models of EAC incidence were built for all-race men and women.

DETAIL

The Phase 1 model family was designed to identify biological mechanisms that may potentially drive the observed EAC incidence trends. In these models, linear or sigmoidal trends for cohort and/or period were applied to one or more biological processes. Thus all individuals of a given age, period, birth cohort, and sex share the same set of biological rates, but these rates may change with birth cohort and calendar year.

The Phase 2 model family extended the Phase 1 models by stratifying the population according to sGERD duration, and then evaluating the mechanistic role of sGERD and OF acting on important biological mechanisms identified in Phase 1. In these Phase 2 models, linear or sigmoidal trends for cohort and/or period were applied to sGERD and OF, which influence biological rates. Individuals of a given age, period, birth cohort, and sex were stratified by decade of sGERD onset, with individuals in each stratum modeled using baseline biological rates before acquisition of sGERD and generally different rates after sGERD onset.



STOCHASTIC SIMULATION COMPONENT

SUMMARY

Carcinogenesis is represented using a multistage clonal expansion model, linking cellular events (division, death, and mutation) to premalignant and malignant clonal growth and cancer detection.

OVERVIEW

The stochastic simulation algorithm (SSA) is a mathematically exact method to follow each event that occurs during a realization of a continuous time Markov chain beginning with a single cell, using cell kinetic parameters fit to SEER incidence data and other sources.

DETAIL

Considering an individual premalignant clone of size X_t at time t , we define the intensity function vector $r(X_t) = (\beta_p X_t, \mu_2 X_t, \alpha_p X_t)$ for death/differentiation, malignant transformation, and birth of new P stem cell, where, over a short period of time s , we expect $r_j(X_t)s + o(s)$ events of type j to occur. Due to the Markovian property of the process, we wait an exponential length of time until the next event occurs with intensity $r_0(X_t) = \sum_{j=1}^3 r_j(X_t) = X_t(\beta_p + \mu_2 + \alpha_p)$. Once an exponential time to next event is chosen, we jump to the neighboring state $X_t + v_j$ with probability $r_j(X_t)/r_0(X_t)$, where v_j is the j^{th} component of the state change vector $v = (-1, 0, 1)$ for the b-d-m process. Fortunately, in the case of the P clone process with constant rates, the probabilities $r_j(X_t)/r_0(X_t)$ are constant with respect to the current state X_t so we may generate a number K of events of the three types with probabilities $(\frac{\beta_p}{\beta_p + \mu_2 + \alpha_p}, \frac{\mu_2}{\beta_p + \mu_2 + \alpha_p}, \frac{\alpha_p}{\beta_p + \mu_2 + \alpha_p})$ and cumulatively sum each $X_t + v^j$ step for the K chosen events to create a state vector $\{ \setminus \text{it } N \}$. Then we generate the K exponential waiting times of the process at once from an exponential with mean $\lambda_t = N(\beta_p + \mu_2 + \alpha_p)$ and cumulatively sum these to arrive at a new later time $t_2 > t$.

The SSA works very well when cell count of the P clone is small and the event intensities $r(X_t)$ are fluctuating quickly. In particular, our simulation benefits to use the SSA for the beginning of a P clone's growth from a single cell, when the probability of extinction is high (β_p is only slightly smaller than α_p) and most clones are eliminated after a small number K of initial events. However, the SSA can become excruciatingly slow when a P clone becomes very large, i.e. contains a large number of stem cells. Therefore, rather than simulating every event choice and time, we can employ an accelerated but approximate procedure called the τ -leap method, first introduced by Gillespie and others.^{1,2,3} The goal of this procedure is to advance the cell count by a preselected time increment τ in contrast to the exponential time increments generated in the SSA. To control the loss of accuracy with this approximation, the choice of leap-size τ must satisfy the historically referenced "leap condition" which is large enough that many events occur in that time, but nevertheless small enough that the intensity function value r is likely to change only "infinitesimally" as a consequence of those events. To the extent that this condition is satisfied, the mathematical rationale in replacing Markovian kinetics with Poisson kinetics⁴ states that the number of times each independent event j will occur in the set time length τ can be approximated by a

FRED HUTCHINSON
CANCER RESEARCH CENTER
A LIFE OF SCIENCE

- Readers Guide
- Model Overview
- Assumption Overview
- Parameter Overview
- Component Overview
- Output Overview
- Results Overview
- Key References



Poisson random variable with mean $\omega(t, t + \tau)$ on the interval $(t, t + \tau)$. For the ordinary τ -leap scheme, we assign $\omega(t, t + \tau) = r_j(X_t)\tau$. Thus, we set the intensity of event j equal to the constant $r_j = r_j(X_t)$ and we update the cell count vector $X_{t+\tau} = X_t + \sum_{j=1}^3 n_j v_j$ where n_j are independent Poisson variates with means $r_j\tau$.

When the stochastic simulation of P clones produces a malignant progenitor M cell, an independent birth–death–detection process for an M clone begins also. This can occur during anytime of surveillance and the malignant clones may employ the same algorithm described above. Considering an individual malignant clone of size X_t at time t , we define the intensity function vector $r(X_t) = (\beta_M X_t, \rho X_t, \alpha_M X_t)$ for death/differentiation, EAC detection, and birth of new M stem cell. The times of ρ events may occur between screens and be counted as a spontaneous, interval detection of EAC.

REFERENCES:

- 1 Gillespie, Daniel T. "Exact stochastic simulation of coupled chemical reactions" in J Phys Chem 1977; 81: : 2340–2361
- 2 Gillespie, Daniel T. "Approximate accelerated stochastic simulation of chemically reacting systems" in The Journal of Chemical Physics 2001; 115: 4: 1716
- 3 Cao, Y.; Gillespie, D. T.; Petzold, L. R. "Efficient step size selection for the tau-leaping simulation method" in The Journal of Chemical Physics 2006; 124: 4: 044109
- 4 Kurtz, Thomas G. "Approximation of Population Processes" in SIAM 1981; : 75



KEY REFERENCES

- Cao, Y.; Gillespie, D. T.; Petzold, L. R.** (2006) Efficient step size selection for the tau-leaping simulation method in *The Journal of Chemical Physics* 124:4, p 044109
- Curtius, Kit, Hazelton WD, Jeon J, Luebeck EG** (2015) A multiscale model evaluates screening for neoplasia in Barrett's Esophagus. in *PLOS Computational Biology* 11:5, p e1004272
- Dent, J., El-Serag, H. B., Wallander, M. A., Johansson, S** (2005) Epidemiology of gastro-oesophageal reflux disease: a systematic review. 54:5, p 710-7
- Falk, G. W., Jacobson, B. C., Riddell, R. H., Rubenstein, J. H., El-Zimaity, H., Drewes, A. M., Roark, K. S., Sontag, S. J., Schnell, T. G., Leya, J., Chejfec, G., Richter, J. E., Jenkins, G., Goldman, A., Dvorak, K., Nardone, G.** (2011) Barrett's esophagus: prevalence-incidence and etiology-origins. in *Ann N Y Acad Sci* 1232, p 1-17
- Gillespie, Daniel T.** (1977) Exact stochastic simulation of coupled chemical reactions in *J Phys Chem* 81, p 2340-2361
- Gillespie, Daniel T.** (2001) Approximate accelerated stochastic simulation of chemically reacting systems in *The Journal of Chemical Physics* 115:4, p 1716
- Hazelton William D., Curtius Kit, Inadomi John M., Vaughan Thomas L., Meza Rafael, Rubenstein Joel H., Hur Chin and Luebeck E. Georg.** (2015) The Role of Gastroesophageal Reflux and Other Factors during Progression to Esophageal Adenocarcinoma in *Cancer Epidemiology, Biomarkers and Prevention* 24, p 1012-1023
- Heberle CR, Omidvari AH, Ali A, Kroep S, Kong CY, Inadomi JM, Rubenstein JH, Tramontano AC, Dowling EC, Hazelton WD, Luebeck EG, Lansdorp-Vogelaar I, Hur C** (2017) Cost-Effectiveness of Screening Patients with Gastroesophageal Reflux Disease for Barrett's Esophagus With a Minimally Invasive Cell Sampling Device in *Gastroenterol Hepatol* S1542-3565:17, p 30197-0
- Kong, C. Y., Kroep, S., Curtius, K., Hazelton, W. D., Jeon, J., Meza, R., Heberle, C. R., Miller, M. C., Choi, S. E., Lansdorp-Vogelaar, I., van Ballegooijen, M., Feuer, E. J., Inadomi, J. M., Hur, C., Luebeck, E. G.** (2014) Exploring the Recent Trend in Esophageal Adenocarcinoma Incidence and Mortality Using Comparative Simulation Modeling. in *Cancer Epidemiol Biomarkers Prev* 23:6, p 997-1006
- Kroep S, Heberle CR, Curtius K, Kong CY, Lansdorp-Vogelaar I, Ali A, Wolf WA, Shaheen NJ, Spechler SJ, Rubenstein JH, Nishioka NS, Meltzer SJ, Hazelton WD, van Ballegooijen M, Tramontano AC, Gazelle GS, Luebeck EG, Inadomi JM, Hur C** (2017) Impact of Radiofrequency Ablation Treatment of Barrett's Esophagus on Esophageal Adenocarcinoma: A Comparative Modeling Analysis. in *Clin Gastroenterol Hepatol* 1542-3565:17, p 30019-8
- Kurtz, Thomas G.** (1981) Approximation of Population Processes in *SIAM*, p 75
- Locke, G. R., 3rd, Talley, N. J., Fett, S. L., Zinsmeister, A. R., Melton, L. J., 3rd** (1997) Prevalence and clinical spectrum of gastroesophageal reflux: a population-based study in Olmsted County, Minnesota. in *Gastroenterology* 112:5, p 1448-56
- Locke, G. R., 3rd, Talley, N. J., Fett, S. L., Zinsmeister, A. R., Melton, L. J., 3rd** (1999) Risk factors associated with symptoms of gastroesophageal reflux in *Am J Med* 106:6, p 642-9

- Rubenstein, J. H., Taylor, J. B.** (2010) Meta-analysis: the association of oesophageal adenocarcinoma with symptoms of gastro-oesophageal reflux in *Aliment Pharmacol Ther* 32:10, p 1222-7
- Ruigomez, A., Rodriguez, L. A. G., Wallander, M. A., Johansson, S., Graffner, H., Dent, J.** (2004) Natural history of gastro-oesophageal reflux disease diagnosed in general practice in *Alimentary Pharmacology & Therapeutics* 20:7, p .751-60.
- Ruigomez, A., Wallander, M. A., Lundborg, P., Johansson, S., Rodriguez, L. A. G.** (2010) Gastroesophageal reflux disease in children and adolescents in primary care. in *Scand J Gastroenterol* 45:2, p 139-146
- SEER** (2010) Surveillance, Epidemiology, and End Results (SEER) Program (www.seer.cancer.gov) SEER*Stat Database: Incidence – SEER 9 Regs Research Data, Nov 2011 Sub (1973–2010)
- Talley, N. J., Zinsmeister, A. R., Schleck, C. D., Melton, L. J., 3rd** Dyspepsia and Dyspepsia Subgroups - a Population-Based Study in *Gastroenterology* 102:4 Pt 1, p 1259-68
- Taylor, J. B., Rubenstein, J. H.** (2010) Meta-analyses of the effect of symptoms of gastroesophageal reflux on the risk of Barrett's esophagus in *Am J Gastroenterol* 105:8, p 1729-37
- Thrift, A. P., Kramer, J. R., Qureshi, Z., Richardson, P. A., El-Serag, H. B.** (2013) Age at onset of GERD symptoms predicts risk of Barrett's esophagus. in *American Journal of Gastroenterology* 108:6, p 915-922
- Wikipedia** (2014) Beta distribution in http://en.wikipedia.org/wiki/Beta_distribution,
-